FINAL REPORT FOR RESEARCH AGREEMENT
#INT-95077-RJVA
"Development of a Riparian Ground Water Model - Banner Creek, Idaho"
CASE WESTERN RESERVE UNIVERSITY
FS Contact: Ms. Carolyn Bohn
CoOp Contact: Dr. Peter Whiting

Development of a three-dimensional groundwater flow model (WaTab3D) and its application at Banner Creek, Idaho

Mikhail Pomeranets
Peter J. Whiting
Department of Geological Sciences
Case Western Reserve University
Cleveland, OH 44106
USA

November 17, 1998

ABSTRACT

The exchange of water, sediment and nutrients between the stream channels and the floodplain is a critical process in riparian lands. In this study we developed a fully three-dimensional groundwater flow model and applied it at Banner Creek, Idaho. At Banner Creek, there is an ongoing investigation of groundwater flow, subsurface chemistry, streamflow and riparian vegetation in a conifer and grassland valley bottom composed of sandy to gravelly alluvium. The three-dimensional model (WaTab3D) simulates the flow in the entire region, including the unconfined layer, and is based on the flow system following the approach proposed by Neuman and Witherspoon (1970a; 1970b; 1971) and Whiting and Pomeranets (1997). The model predicts flow from the areas of highest elevation on the eastern edge and northeastern corner of the study area toward the channel on the western edge of the study area. Velocity vectors generally decrease with time at a location. In general, the vertical component of flow is downward over much of the study area. Velocity vectors are often relatively large near the channel and generally downward and toward the channel, indicating that the valley bottom is contributing water to the channel. These predictions are consistent with the observed piezometric surface and its evolution.

INTRODUCTION

The National Research Council in their report Opportunities in the Hydrologic Sciences (1991) identified a number of unsolved problems in hydrology. Among the frontier issues was the question 'How are water, sediment, and nutrients exchanged between river channels and their floodplains?' One critical piece of an answer to this question is an understanding of the connection between channel water and shallow groundwater of the floodplain.

Floodplain soils have been described as sponges (National Research Council, 1991) which soak up water in addition to pollutants and nutrients. In a flood, substantial quantities of water are in detention storage as overbank flows. A portion of this water infiltrates the floodplain soil during such overbank events or whenever channel water level is higher than the water table in the stream bank. Our analysis suggests that up to perhaps 0.4 percent of the annual water yield can be temporarily stored within the soil of the floodplain and when peak flows occur after long periods of baseflow, as for instance in snowmelt-dominated regions, up to 2 percent of the hydrograph volume may be stored in the floodplain soil (Whiting and Pomeranets, 1997). The storage of water in floodplain soils should diminish peak flood volumes (Ponce, 1991) and flood heights, but the magnitude of this effect is poorly quantified. Nonetheless, it is clear that transfer of runoff to storage in floodplain soils on the rising limb of the hydrograph will serve to delay runoff, and release of water from storage in the soils will sustain stream discharge on the falling limb of the hydrograph.

Stream baseflow in late summer and fall is maintained by shallow groundwater. One major source of these flows is water stored temporarily in the floodplain and wetland (Kondolf et al., 1987). The release of water from the floodplain soils serves to increase the magnitude and duration of low flows, maintains instream flows and water temperatures necessary for adequate and diverse fish populations, and maintains the moisture regime sustaining riparian vegetation (Ponce, 1989). Several studies have shown how channel incision, which decouples the channel from its floodplain, results in decreased late season channel flows. Winegar (1977) described how overgrazing at Camp Creek destabilized banks and led to channel incision. A grassy wetland on the floodplain was converted to a sage-dominated surface as the water table was lowered beyond the reach of herbaceous plants. Channel flow became intermittent after incision. Recent efforts to exclude livestock at the site have led to channel aggradation and increases in water stored in the bank, and the channel has been converted back to a perennial stream (OSU-Water Resources Institute, 1986). There are other reports of the alteration in flow regimes associated with landuse (Ponce, 1989).

The floodplain and associated wetlands are often called the 'kidneys' of the landscape. The redistribution of pollutants and nutrients by shallow groundwater flow afford opportunities for transforming and immobilizing pollutants, nutrients and sediments (Peterjohn and Correll, 1984). The vast majority of these substances will be delivered to the floodplain from the adjacent valley sides and surrounding landscape as surface runoff or shallow groundwater flow, or will be delivered to the floodplain from the channel either as infiltrating overbank flows or as seepage through the streambank. Chemical reactions which transform and immobilize pollutants and nutrients occur in the floodplain soils because of the potential for long contact times, the presence of reactive media (organic materials or mineral soils), and commonly anaerobic conditions. For example, because denitrification depends on anaerobic conditions, riparian soils are important sites of nitrate removal from groundwater. Higher phosphorus availability under anaerobic conditions, combined with productive riparian communities, allows for greater phosphorus retention through plant intake (Green and Kauffman, 1989).

The evolution of the water table in the nearbank region has several important physical and ecological ramifications. The stability of the channel bank is controlled in large measure by the magnitude of pore pressure developed in the bank. The pore pressure is controlled by the water level in the bank relative to the channel water level. If channel water level drops rapidly or soil texture does not allow free drainage, stream banks, particularly steep banks, may collapse. Riparian vegetation depends on the depth to the water table and the rate at which the water table drops. Several species are rooted below the water table and other species such as cottonwoods, are said to germinate and survive to seedlinghood only if root growth can keep pace with the drop in the water table after the flood hydrograph (Moss, 1938; Wilson, 1970). The structure of riparian plant communities is determined largely by the surface and groundwater hydrology connected with streams. In turn, riparian plant communities play a major role in structuring fish and wildlife habitat in the riverine ecosystem. The

understanding of the biological processes in these riparian zones requires an understanding of the hydrology in the hyporheic zone -- a point emphasized by Bencala (1993).

One approach to the development of an understanding of the connection between channel water and shallow groundwater of the floodplain is modeling. There are a number of widely used groundwater models based on different approaches and techniques which are capable of solving various problems in two or three dimensions. Most of these models, such as MODFLOW (McDonald and Harbaugh, 1988), PLASM (Prickett and Lonnquist, 1971), AQUIFEM-1 (Townley and Wilson, 1980) are designed for extensive regions. Three-dimensional finite difference MODFLOW can work in both the aquifer and the flow system mode for confined regions, but relies upon the Dupuit assumptions in unconfined subregions (Anderson and Woessner, 1992). Two-dimensional finite difference PLASM and finite element AQUIFEM-1 are aquifer models. Because the free surface is the most difficult boundary to treat and will be involved in our model, we will limit the technical discussion of the models to the way they deal with the unconfined regions.

The Dupuit assumptions underlying the aquifer models reduce the problem's dimension by one; for example, for the three-dimensional flow regions, head becomes dependent only on the two horizontal coordinates. The two-dimensional Boussinesq equation (Bear, 1972; Anderson and Woessner, 1972) must be solved instead of the 'full' three dimensional equation underlying the flow system models. By using the Dupuit assumptions, one avoids the difficulties associated with dealing with the free surface: mathematically, the free surface is no longer a boundary of the problem's domain that is unknown *a priori* and needs to be obtained as part of the solution. Instead, the elevation of the free surface on each vertical is simply taken equal to the value of head for this vertical after heads are calculated. Consequently, models based on the Dupuit assumptions do not solve rigorously for the seepage surfaces (Anderson and Woessner, 1992). MODFLOW, PLASM and AQUIFEM-1 identify the seepage surface wherever the free surface exceeds some prescribed limit (normally the land surface).

The models using the Dupuit assumptions have several inherent disadvantages, of which the most obvious is not allowing for the vertical component of flow. This may often lead to paradoxical situations, such as when a point source does not affect the horizontal direction of the streamlines, no matter how intense is the source. A significant error can occur when the calculated velocities are used for particle tracking. Because the hydraulic conductivity is vertically-averaged, vertical anisotropy often cannot be represented adequately; for example, inclusion of different conductivity will be 'uniformly distributed' from top to bottom of the flow region. Also, there is a problem with representing dipping aquifers (Anderson and Woesnner, 1992). Another limitation stemming from the Dupuit assumptions is that the significantly-sloped free surface (e.g., near water reservoirs) is poorly predicted. Good prediction of the water table near such reservoirs (rivers, lakes, wetlands, etc.) is often a key issue in the study of the connectedness of surface and subsurface water.

While the aquifer models give an acceptable approximation of the flow for regions with horizontal dimensions far greater than vertical dimensions, it is often preferable to use the flow system models for less extensive regions where vertical gradients may be important and near features responsible for high vertical gradients (channels, wells in unconfined aquifers, etc.). An example of a flow system model is FREESURF (Neuman, 1976) which is capable of handling steady-state profile flow (two-dimensional and axisymmetric). This finite element code is based on a technique proposed by Neuman and Witherspoon (1970a; 1970b). The transient profile version also exists based upon later work (Neuman and Witherspoon, 1971). The technique permits one to solve rigorously for the free surface of any configuration and easily treats any kind of heterogeneity and anisotropy simply by prescribing different properties to individual elements. The flow system models are more difficult to implement, but they eliminate the important disadvantages associated with the Dupuit assumptions. For treating the free surface, finite elements are best suited (Anderson and Woessner, 1992). The free surface is obtained iteratively, and the element mesh is allowed to deform to accommodate the changing geometry of the flow region. The multiple aquifer extension of AQUIFEM-1, AQUIFEM-N (Townley, 1990), uses the similar technique for determining the position of the free surface in the profile mode, while still using the Dupuit assumptions in the three-dimensional mode (Anderson and Woessner, 1992).

When solving the nonlinear Boussinesq equation underlying aquifer models, MODFLOW, PLASM, and AQUIFEM-1 in effect linearize the equation by using the current value of the saturated thickness (Anderson and Woessner, 1992). For example, in nonsteady problems, such an approach means that all quantities on the new time step are calculated using the aquifer transmissivity (hydraulic conductivity times saturated thickness) that existed on the previous time step. This may create an additional error (besides that associated with the Dupuit theory) unless sufficiently small time steps are used. On the contrary, in the Neuman and Witherspoon (1971) method, the water table is calculated iteratively as part of the solution for each time.

We are not aware of any available three-dimensional model that simulates the flow in the entire region, including the unconfined layer, based on the flow system viewpoint. Our intent, as we will develop it during the remainder of the report, was to create such a three-dimensional flow system model (WaTab3d) following the approach proposed by Neuman and Witherspoon (1970a; 1970b; 1971) and Whiting and Pomeranets (1997) and to apply this model as part of a multidisciplinary study of surface water and groundwater connections at Banner Creek, Idaho.

DEVELOPMENT OF WaTab3D

Mathematical modeling may be subdivided into three major steps: (1) selecting a model based on purposes of modeling and physical circumstances, (2) resolving the model by some mathematical method, and (3) verification of the model. Below is an explanation of these steps as they were employed in our model (WaTab3D) which builds upon our earlier 2-dimensional work (Whiting and Pomeranets, 1997) (WaTab2D).

Selecting a model

The focus of our modeling is the saturated flow in an aquifer adjacent to a channel. The dominant feature of the flow responsible for a major portion of complexity in the model is the changing free surface, or water table. Even a steady free surface presents a major difficulty for a modeler.

Most widely known groundwater modeling packages designed to treat very extensive regions (MODFLOW, AQUIFEM-1, AQUIFEM-N) make use of the simplifying Dupuit assumption (e.g., De Wiest, 1965) when dealing with a free surface (Anderson and Woessner, 1992). According to the Dupuit assumption, head is constant along any vertical cross-section. This approach reduces the problem's dimension by one but has limitations, such as not accounting for the vertical component of the seepage velocity and poor prediction of a significantly sloped free surface.

We used an exact traditional model describing time-dependent unconfined (i.e., with a free surface) saturated groundwater flow, which is a free moving boundary problem (e.g., Bear, 1972, Polubarinova-Kochina, 1962, Freeze and Cherry, 1979). Here is the universal mathematical model in notations used by Neuman and Witherspoon (1971):

$$\frac{\partial}{\partial x_i}\left(K_{ij}\frac{\partial h}{\partial x_j}\right)=S_s\frac{\partial h}{\partial t} \tag{1}$$

$$h(x_i,0)=h_0(x_i) \tag{2}$$

$$x(x_1, x_2,0) = x_0 (x_1, x_2) \tag{3}$$

$$h(x_i, t)=H(x_i, t) \quad \text{on prescribed flux boundaries} \tag{4}$$

$$K_{ij}\frac{\partial h}{\partial x_i}n_i = -V(x_i,t) \quad \text{on prescribed flux boundaries} \tag{5}$$

$$\xi(x_1, x_2, t) = h_0(x_1, x_2, \xi, t) \quad \text{on free surface} \tag{6}$$

$$K_{ij}\frac{\partial h}{\partial x_j}n_i = \left(I - S_y\frac{\partial \xi}{\partial t}\right)n_3 \quad \text{on free surface} \tag{7}$$

$$h(x_i, t) = x_3 \quad \text{on seepage face} \tag{8}$$

The governing equation (1) results from the equation of conservation of mass combined with Darcy's law (Bear, 1972). The latter has the following form:

$$q_j = -K_{ij}\frac{\partial h}{\partial x_i}$$

where q_j are the components of the specific discharge vector, h is piezometric head, K_{ij} are the components of the hydraulic conductivity tensor, and x_i are the Cartesian coordinates (x_3 is vertical). t is time and S_s is the specific storativity which is usually set to zero for the unconfined flow when the region of interest does not include a confined subregion. The equations (2) and (3) are the initial conditions specifying, respectively, the distribution of head and the location of the free surface at the initial moment, t=0. The letter ξ stands for the elevation of the free surface. The rest of the equations are the boundary conditions. Equation (4) specifies the value of head on the boundaries on which head can be either measured or determined based on the topography. For example, on a vertical or sloped boundary with a water reservoir head is constant, and H in this case represents the elevation of the water level in the reservoir. Values of h, H, and ξ are measured with respect to the same horizontal datum. Equation (5), where V is the specific flux, is set for the boundaries on which flux can be determined a priori. For example, V=0 on impervious boundaries. Because the exact location of the free surface is unknown and is a part of the solution, two boundary conditions should be specified on the free surface. Equation (6) results from the fact that pressure is atmospheric (zero) on the free surface. Equation (7) specifies fluxes on the free surface, where I represents infiltration to, or evapotranspiration from, the free surface, and S_y is the specific yield. For a steady free surface with no infiltration or

evapotranspiration, the right-hand side of (7) becomes zero, and the equation is that of a stream line. Similar to (6), equation (8) is the condition of atmospheric pressure on the seepage face.

Method of solution

A numerical technique proposed by Neuman and Witherspoon (1970a, 1970b, 1971) was selected to resolve the boundary value problem presented above. Because the method is very well known and available in original papers and is further described in Whiting and Pomeranets (1997), we will give only the key points here. The technique utilizes the principles of the finite element method, that is the minimization of a problem's functional (incorporating both the governing equation and the boundary conditions) over the problem's region which is subdivided into a mesh of finite elements. An iterative procedure is used at each time step for determining the exact location of the free surface and, consequently, the length of the seepage face. Each iteration is divided into two steps during which the location of a free surface is fixed. On the first step, both the free surface and the seepage face are treated as prescribed head boundaries. On the second step, they are treated as the prescribed flux boundaries using the known fluxes on the free surface along with the fluxes calculated during the first step on the seepage face. At the end of the iteration, the free surface is shifted to a location that is believed to be its best approximation, based on the values of head calculated during the second step. Then the iterations continue until a satisfactory position of the free surface is reached.

Realization

The method of Neuman and Witherspoon, although described in detail in the original papers for two-dimensional (2D) problems, is applicable to general three-dimensional (3D) problems. However, managing 3D regions is a much more complex task than managing 2D regions. It is no longer practical to work with tetrahedral elements (analogous to triangular elements in 2D that were used for implementation of the earlier WaTab2D (Whiting and Pomeranets, 1997)). Instead, for WaTab3D we used isoparametric 8-node and 20 -node elements. An isoparametric element is defined in the auxiliary space (u, v, w), where it is a cube extending from -1 to 1 in each direction. An 8-node element only uses vertices for the nodes, while a 20-node element has an additional node in the middle of each cube's edge. If both types of elements are used simultaneously, some "transitional" elements have a different number of nodes --- between 8 and 20.

The idea of using isoparametric elements defined in the local space is to make up for the irregularity of the problem region. The region in the isoparametric space always consists of a set of regularly-shaped elements, each defined in its own space varying between -1 to +1 in each dimension. A set of interpolating (or mapping) functions is defined for each element, one function per node, to map any point in the local space onto the global, real-life space. That is, the individual properties (shape and

location of each node) show up in the mapping functions. In the general form, the mapping can be defined like this:

$$x = \sum N_i(u,v,w)x_i$$

where N_i are interpolating functions, and x_i are coordinates of the element's nodes in the global space.

A similar formula applies to functions, e.g., head, first calculated in the local space of each element, is mapped like this:

$$h(x,y,z) = \sum N_i(u,v,w)h_i$$

where N_i are the *same* interpolating functions as used for mapping coordinates, and h_i are the values of the head at the nodes. Use of the same interpolating functions for mapping physical points and functions lies at the heart of the isoparametric techniques.

3D isoparametric elements with 8 nodes (one at each corner) define linear interpolations: edges of the corresponding elements in the physical space are straight-line segments, and functions within those elements are distributed linearly. 20-node (an additional node in the middle of each edge) elements define quadratic interpolations: edges of the physical elements are parabolic and functions are quadratically interpolated by their nodes' values. Transitional elements are degenerated from the 20-node elements by omitting mid-nodes at some edges. Mathematically, N_i is set to zero for the missing locations. The edges with the omitted mid-nodes will be straight-line segments.

The mapping relationships for the target function's first derivatives are more complex. First derivatives of head, for example, participate in the representation of the velocity-related quantities, such as discharge or velocity itself. An inverse of the Jacobian matrix (see, e.g. Kazda, 1990) is used for transformation of the first derivatives defined in the local space (readily calculated) to the first derivatives defined in the global space, which are used in the differential equations. The Jacobian matrix is calculated in every element's node, then inverted and used for calculation of global derivatives. The Jacobian (a Jacobian matrix' determinant) is used also to ensure that the elements have a permissible shape: at any node the Jacobian should always be positive (Kazda, 1990). We used this condition to ensure that all our mesh deformations are physically consistent.

Internal mesh organization

To deal with the 3D element mesh of constantly changing geometry (as the water surface moves with time), as well as to facilitate prescription of the initial geometry and the boundary

conditions, we have developed an original technique, which we are describing below.

The essential idea of our technique is to have two meshes of elements: a mesh of shell elements and a mesh of working elements. The shell elements are responsible for the 'given' properties of the region: physical geometry, material properties (conductivity, specific storage, specific yield), and boundary conditions. Those are prescribed by the user. A shell mesh can have only as many shell elements as necessary for sufficiently accurate representation of the physical conditions. The ultimate case is one shell element. Each shell element is subdivided into a number of working elements to yield the working mesh. The user controls the density of the working mesh by specifying the number of subdivisions along each of three directions. The shell is automatically subdivided into a mesh of working elements. The working elements are those participating in the mathematical solution; their number determines the accuracy of the results. The working mesh is the one used to solve the problem. It deforms following the movement of the water table, which forms the top of the working mesh. The shell elements do not move.

Both shell elements and working elements are normal isoparametric elements that use the above transformations for mappings from the local space to the global space. However, the working elements have one more coordinate space: the local space of the shell element that currently contains this working element. As the mesh deforms, the working elements are moving within the shell elements; in the process, they can change their host shell element, 'flowing' from the local space of one shell element to its neighboring shell element. A working element keeps track of its movement within the mesh of shell elements: at any moment, a working element knows its host element and its own coordinates in the local space of the host. Since the boundary conditions and the material properties are tied to the shell elements, on each time step a working element determines also its characteristics based on the properties of the current host shell element.

As a result of the approach, we achieve greater generality and convenience:

(1) We do not have to make sure that individual elements will stay within a layer of initial material properties (very often a traditional constraint). It is much more convenient to assign all properties to stationary big elements. Each moving working element is automatically aware of its current properties; and

(2) We do not have to worry about mesh leaving physical boundaries during its deformation, since the working mesh cannot possibly go beyond the shell mesh, which specifies the physical boundaries. That is, even though the working elements know nothing about the site geometry, their movement can be effectively controlled through just a few (maybe even one) prescribed shell elements.

Verification of the model

We compared the solution given by our model with the results published by Rushton and Redshaw (1979). They used a finite-difference method with a specially formulated boundary condition on the free surface. The region was two-dimensional vertical profile square dam of uniform permeability, with water on each side of the dam.

With our model, we simulated the Rushton and Redshaw situation by specifying a parallelepiped dam so that its vertical cross section had the exact geometry of that given by Rushton and Redshaw. The boundary and initial conditions were chosen symmetrical relative to the cross-section so as to duplicate the conditions used by Rushton and Redshaw. Results from our analysis yielded a symmetrical water surface with a profile practically coinciding with that given by Rushton and Redshaw.

SITE CHARACTERISTICS

The study site is along Banner Creek in the Boise National Forest, Idaho at an elevation near 5300 feet (1620 m). Much of the annual precipitation falls as snow and the snowmelt is typically the dominant hydrologic event of the year. Banner Creek drains into the Crooked River which drains into the North Fork of the Boise River.

At this site the US Forest Service has installed instrumentation in a portion of the valley floor and channel to examine the connectedness of surface water and groundwater along a mountain stream and to examine the temporal changes in water chemistry in part associated with vegetative uptake. A US Geological Survey gage measures the discharge of Banner Creek above the study area. Precipitation, wind speed, and temperature are recorded by the US Forest Service at the site. A total of 24 piezometers were installed. Tensiometers were placed near each piezometer. The piezometers and tensiometers are contained in four transects that extend from the channel to the left valley wall. One piezometer in each transect is in the bed of the channel. Data from the piezometers are stored on recorders every hour. Additional wells (about 20) have been drilled for retrieving water samples. These wells provide additional information on the piezometric surface. Water temperature, specific conductivity and pH are measured. Water samples are collected weekly during the spring and summer and less frequently at other times. Water is analyzed for nitrogen (ammonia, nitrate, total nitrogen), phosphorus (dissolved and total), total organic carbon, major cations (Na, Mg, Ca, K), strong acid anions (F, Cl, NO_3, PO_4, SO_4), ferous/ferric iron, silica, and other constituents.

Banner Creek at the site meanders through a 150 meter wide valley floor containing a mosaic of conifers, shrubs and grassland. The gravel-bed channel is about 5 meters wide. The study area

extends roughly 65 m from the left side of the valley (as viewed looking downstream) to the channel and along the valley bottom for about 140 m (Figure 1). The highest elevations are in the northeast corner of the study area on the distal part of an alluvial fan associated with an intermittent draw draining the valley side. The topography of the valley floor in the upstream part of the study area slopes from the alluvial fan toward the channel. Toward the lower end of the study area, there is a larger downvalley component to the slope of the valley floor. The lowest elevations in the study area are along the stream channel. The valley floor preserves some evidence for the migration of the stream channel. There are subtle curvilinear depressions near traverse 3 that we interpret to be old meander scars. Soils are generally sandy to gravelly granitic alluvium in the study area. In some parts of the study area, particularly near the meander scars, are found organic rich zones. Hydraulic conductivity ranges from 5.0×10^{-5} m s^{-1} to 4.0×10^{-3} m s^{-1} although the largest numbers seem to reflect macropore flow (J. Clayton, personal communication, 1997). The average hydraulic conductivity of 4.0×10^{-4} m s^{-1} is typical of sand.

During the spring and summer of 1996, US Forest Service personnel collected data on the piezometric response in the valley bottom materials. Figures 2a-e present contour maps of the elevation of the piezometric surface on the following days - 29 April, 29 May, 26 June, 11 July, and 7 August 1996. On 29 April (Figure 2a), the water table slopes steeply westward (relative to the later dates) from the eastern and northeastern portions of the study area toward the channel. On 29 May (Figure 2b), the water table slope has relaxed and, except upstream of traverse 2, there is a larger component of downvalley flow. The flow direction in this area is at about 45° to the general trace of the channel and valley axis. By 26 June (Figure 2c), the slope of the piezometric surface is primarily downvalley except along the eastern edge of the study area, at the base of the valley side. The water table geometry is largely unchanged on the last two dates for which data are available - 11 July and 7 August (Figures 2d and 2e) Over the period of monitoring presented, the range in the elevations of the water table in the study area decreased from 4.0 m to 2.5 m (Table 1). Since the maximum water table elevations are seen

Table 1 - Elevation of the water table in the study area

DATE	Maximum elevation (m)	Minimum elevation (m)	Difference (m)
29 April 1996	1621.4	1617.4	4.0
29 May 1996	1620.5	1617.4	3.1
26 June 1996	1619.7	1617.1	2.6
11 July 1996	1619.5	1617.0	2.5
7 August 1996	1619.4	1616.9	2.5

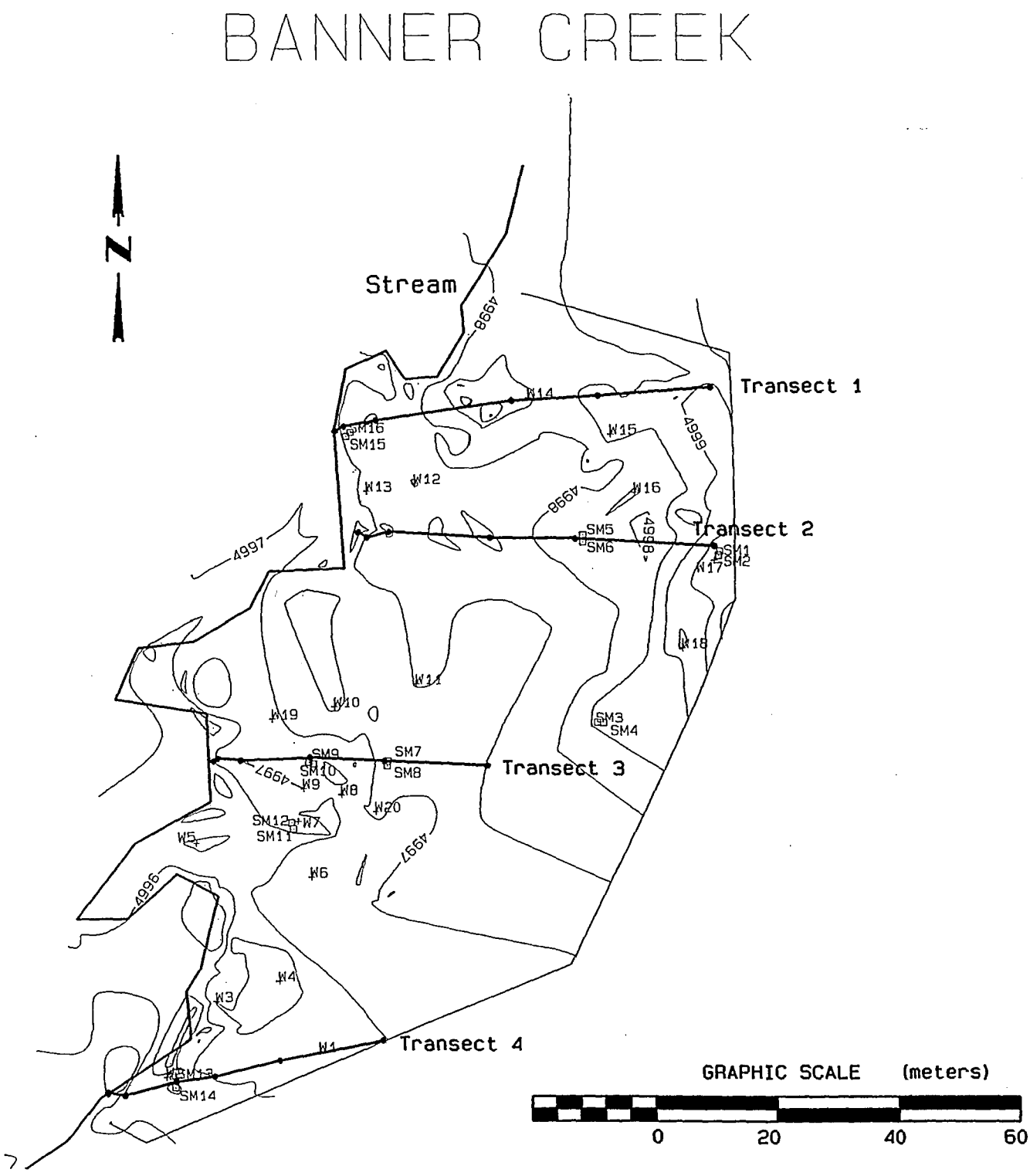

Figure 1 - Topographic map of the site including locations of piezometers and tensiometers.

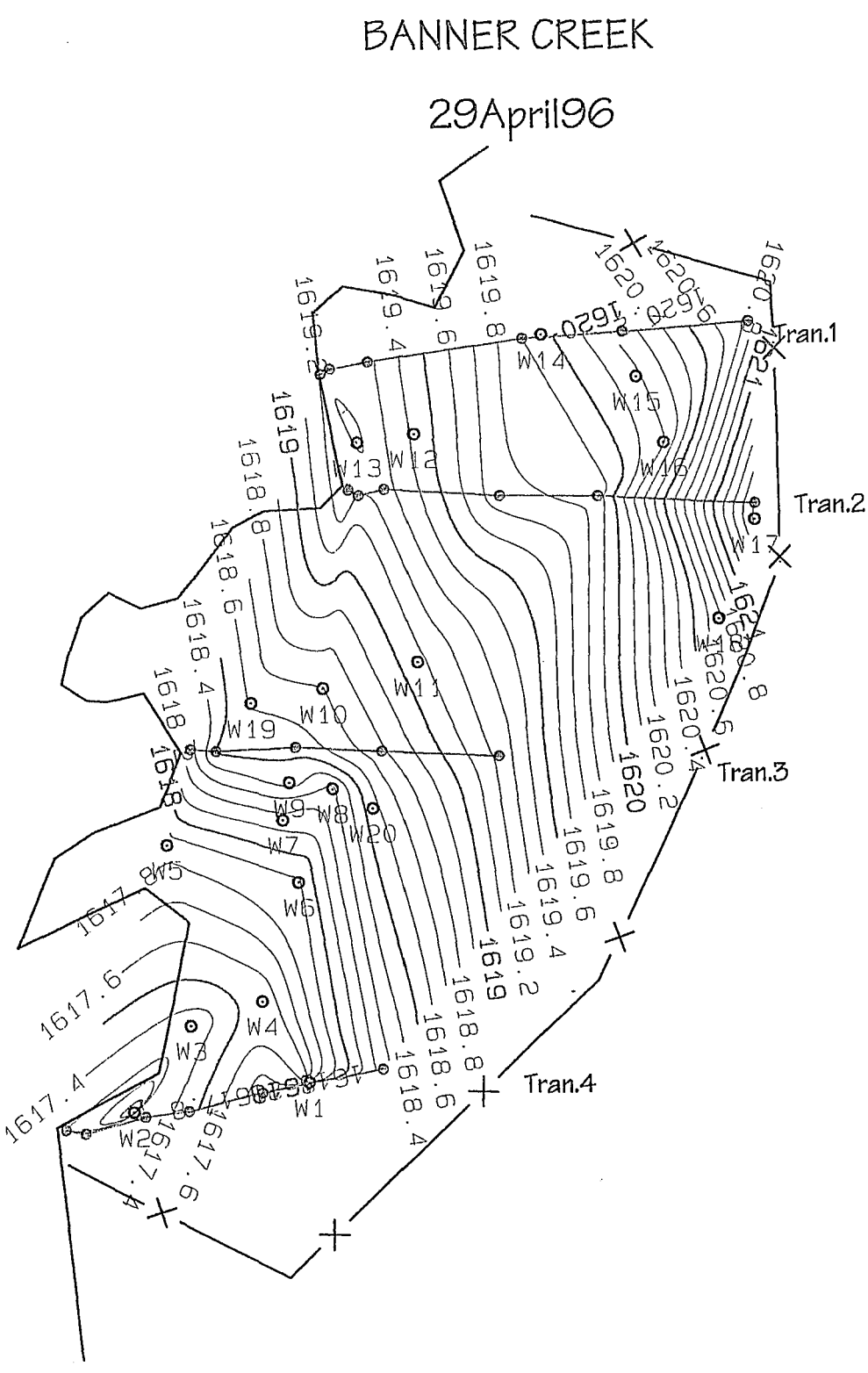

Figure 2a - Contour maps of the elevation of the water table on 29 April 1996.

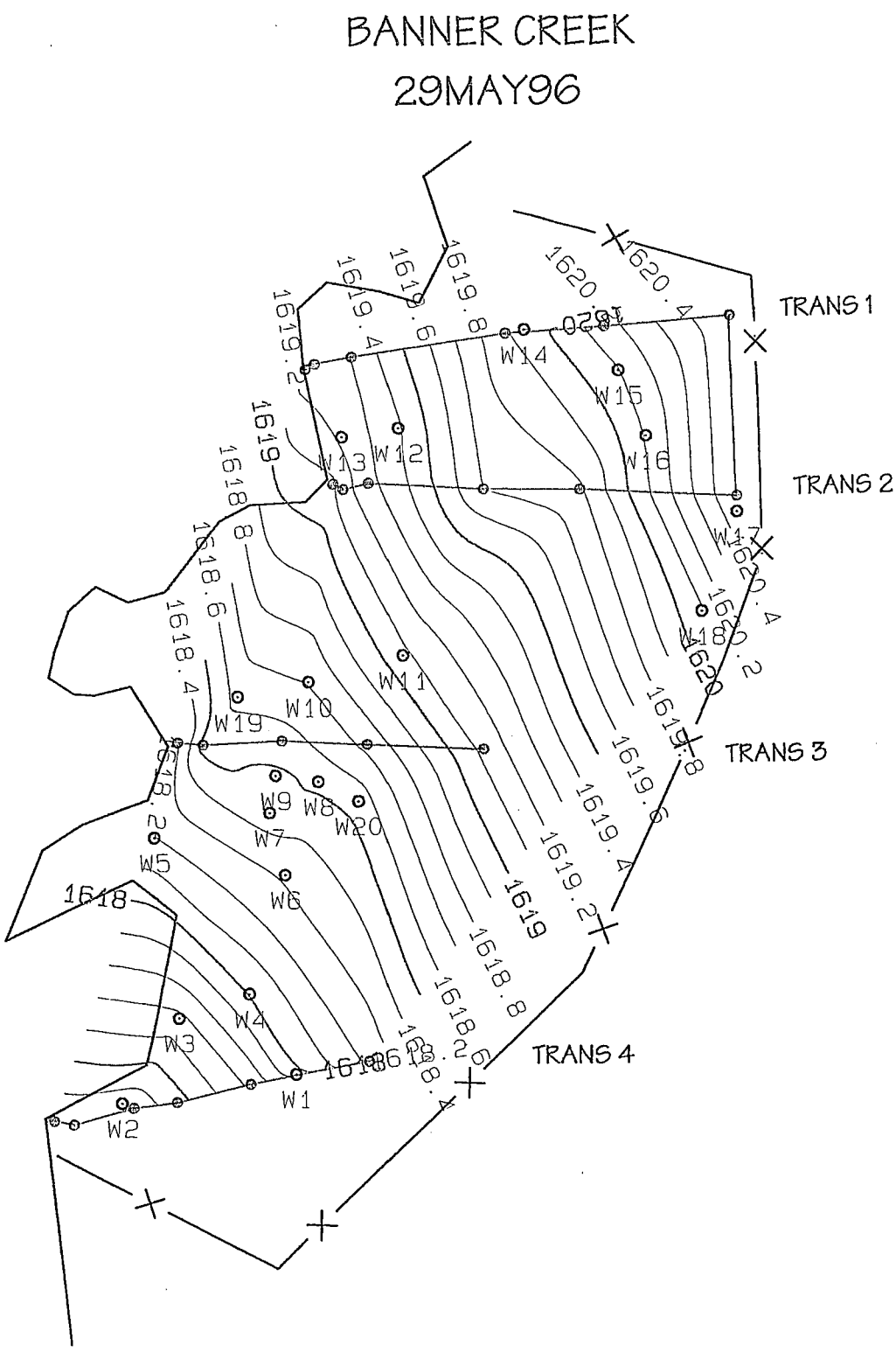

Figure 2b - Contour maps of the elevation of the water table on 29 May 1996.

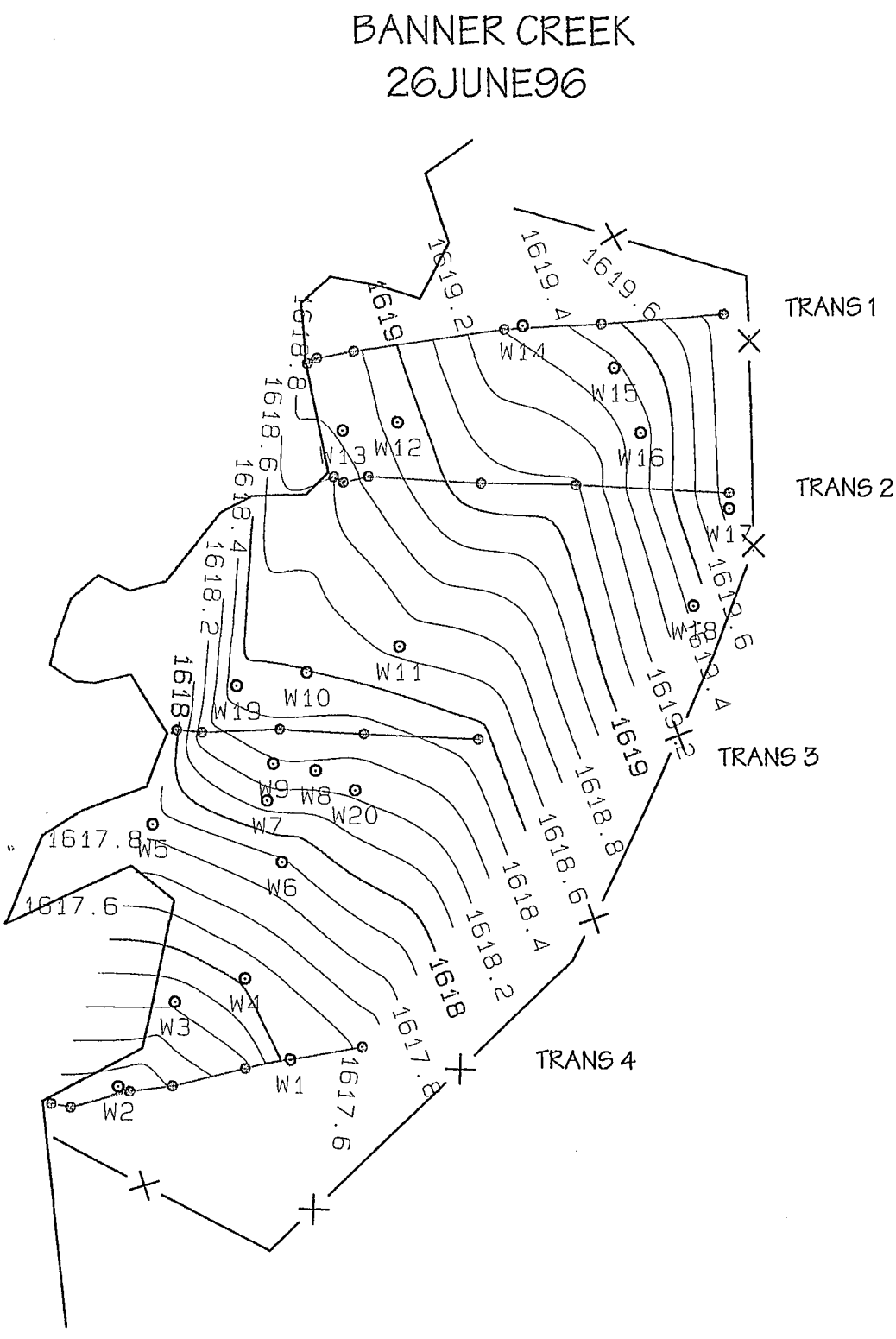

Figure 2c - Contour maps of the elevation of the water table on 26 June 1996.

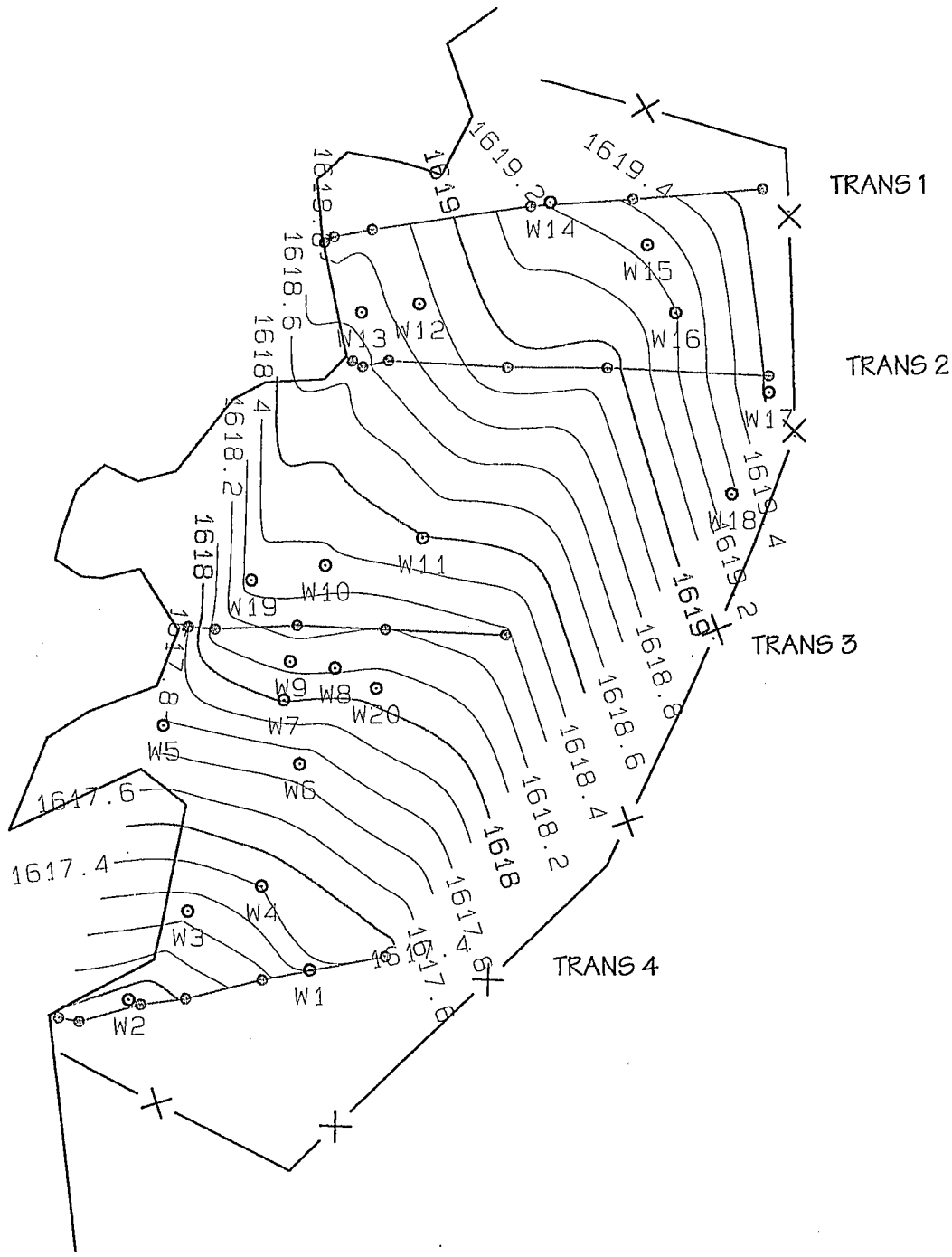

Figure 2d - Contour maps of the elevation of the water table on 11 July 1996.

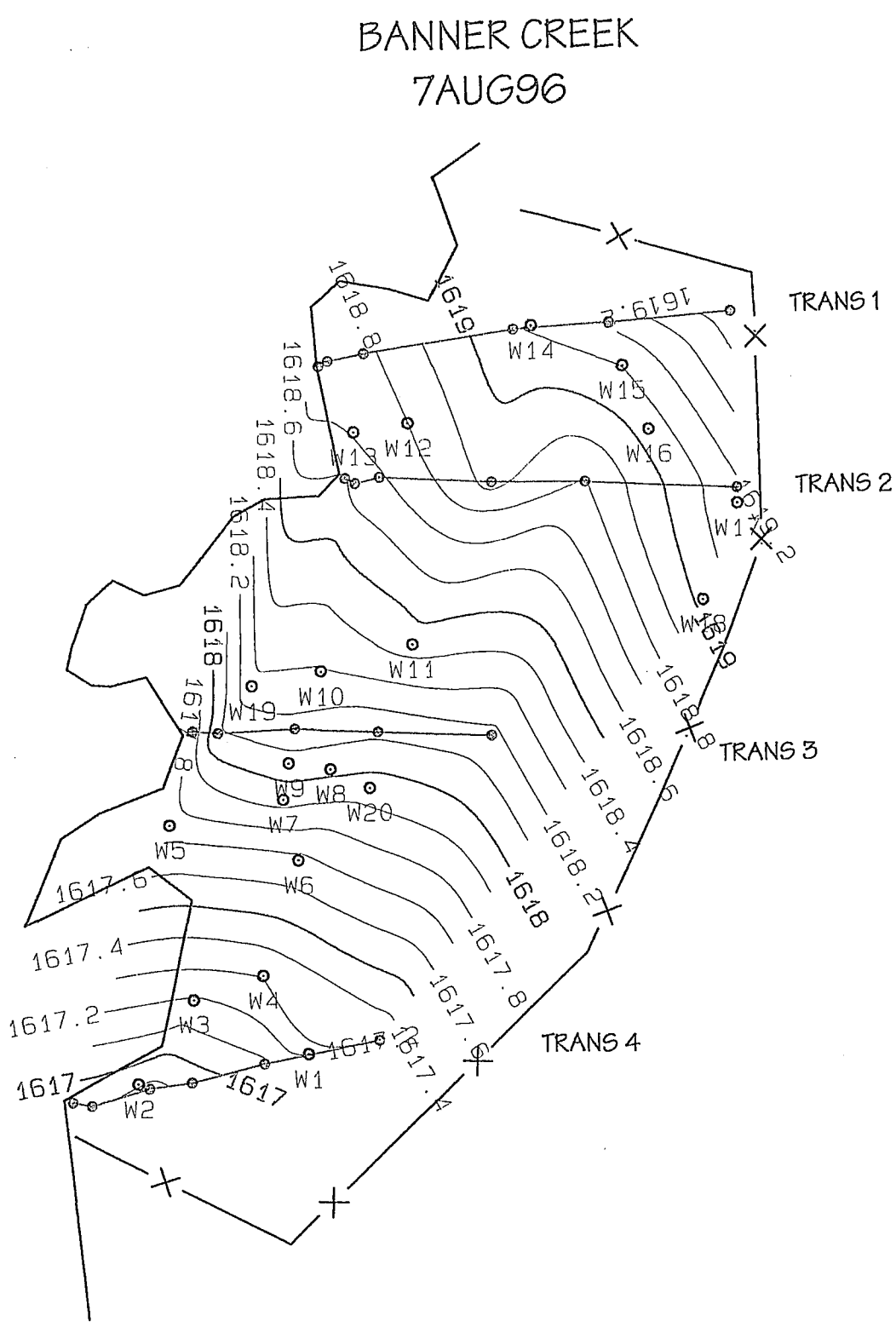

Figure 2e - Contour maps of the elevation of the water table on 7 August 1996.

in the northeast corner of the study area, and the lowest elevations in the southern downstream parts of the study area, the change in the maximum or minimum elevations over time describe local changes in water level as well. Over the period of study, the water table in the northeast part of the study area dropped 2.0 m. The corresponding drop in the water table along the stream at the downstream end of the study area was only 0.5 m. The change in the water table along the channel in the upstream part of the study area was also 0.5 m over this period so it appears that much of the decrease in range (from 4.0 to 2.5 m) is associated with transient contributions to the alluvial fan in the northeast corner of the study area.

MODEL APPLICATION AT BANNER CREEK

We subdivided the study area into a mesh of 19 shell elements based on the planar geometric outline of the region. Figure 3 presents the planform view of the shell mesh (thick lines) and the working mesh (thin lines). It was sufficient to have only one vertical layer of the shell elements (that is, each individual shell element extends across the entire depth of the problem region). All shell elements have 8 nodes. For the calculations presented below, each shell element was subdivided into 27 working elements (3 by 3 along each horizontal directions and by 3 along the vertical direction), yielding the working mesh of 513 elements. As can be seen from the figure, the shell elements become smaller near the river. Consequently, the working mesh is much finer in that area, too.

The period for which data on the piezometric surface was available, 29 April to 7 August 1996, was modeled. The information from 29 April (day 0) was taken as the initial condition (see discussion of this situation later, in the section (Accuracy of the results)). The elevation of the water table was read from the piezometric map for that day (Figure 2). For all later times, the position of the water table was calculated as part of the solution of the system of differential equations.

Boundary conditions were also read from the map of 29 April 1996 and prescribed at those nodes of shell elements that lie on the region boundaries. At each node, the values at each moment were assumed to vary linearly between values for this node available from the maps for the discrete dates. For the presented calculations, all boundaries were assumed to have prescribed-head conditions (head is changing with time but is known), except a linear-segment boundary stretch along the shell elements # 1 and # 2 (the one nearly perpendicular to the river), which was assumed to be a zero-flux boundary.

The material properties for the presented results were prescribed as follows. Hydraulic conductivity was taken as 200 m/d within all shell elements except elements # 4,3,8,7,10,0,16,17, where it was taken as 400 m/day. See Figure 3 for the location of these elements. Assigned hydraulic conductivities are based upon reported values measured on 13 October 1995 with constant head tests

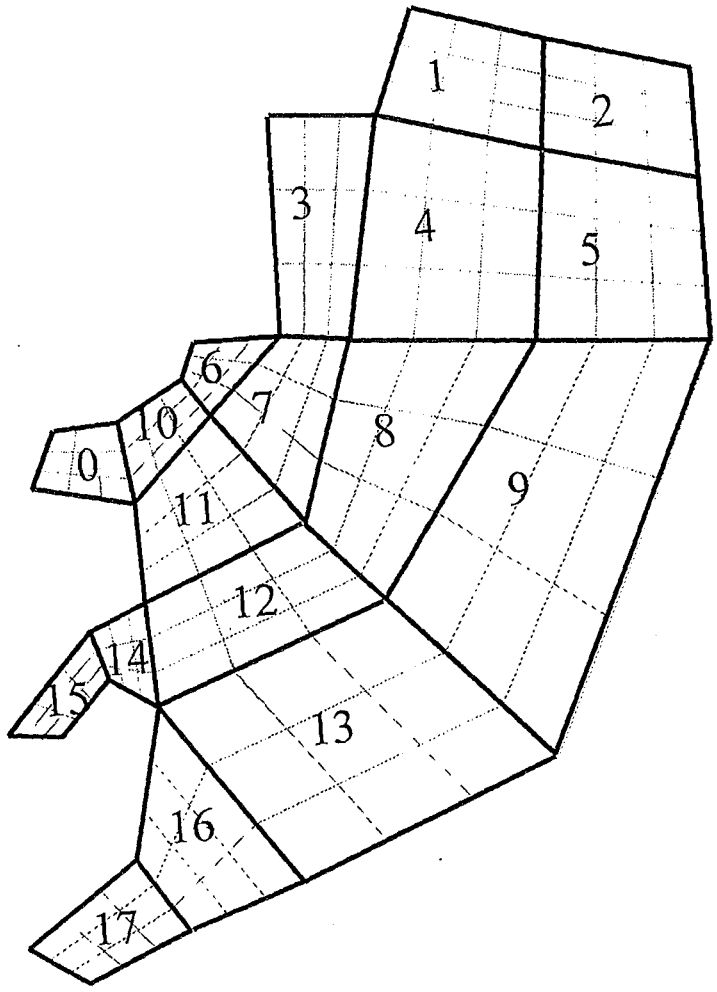

Figure 3 - Planar view of the map mesh including element numbers.

(James Clayton, personal communication, 1997). Specific storage was taken as 0 everywhere; specific yield was taken as 0.5 again everywhere. (*See also the discussion in the section Accuracy of the results.*)

Results of the calculations are shown as the velocity field on various dates (Appendix A). Velocity vectors are three-dimensional, so the figures show only their projection on the horizontal plane. However, downward vectors are shown in solid lines, with closed heads; whereas the upward vectors are shown in dashed lines, with open heads. The stand-alone arrow at the bottom of the pictures shows the scaling: the length of the arrow represents a velocity of 26.4 m/d. In order not to clutter the pictures, contours of only the shell elements are shown (rather than those of the working elements, in which velocity was actually calculated).

Velocity was calculated in the Gaussian points (Kazda, 1990), that do not lie exactly on the elements' boundaries, but on some distance from them. For the used scheme of 2 by 2 by 2 Gaussian points in each direction, the distance is equal to 0.577 in the isoparametric space. Calculated in the Gaussian points, velocity is more accurate than if calculated in the elements' nodes, where it is not continuous (Kazda, 1990).

For each date, the velocity fields in six successive layers were calculated (three working elements across the depth with 2 Gaussian points each), each layer consisting of the respective Gaussian points of each working element (Figure 3). Layer 0 is the closest to the water table, layer 5 is the closest to region's bottom. The actual elevation of the successive layers varies as the water table shifts in time.

DISCUSSION

Patterns of flow

The evolution of the flow fields in time and with depth are shown in Appendix A. For the purposes of discussion, we will focus on the results from days 30, 60, and 90 (Figure 4a-c). There are two reasons for the attention to these dates: first, they provide a good characterization of the evolution over the season, and second, because these specific dates avoid, to the degree possible, a problem of timestep sensitivity.

WaTab3D predicts flows at all levels that are generally from the areas of highest elevation on the eastern edge and northeastern corner of the study area and toward the channel on the western edge of the study area as would be expected given the vertically uniform and spatially largely uniform hydraulic conductivity. Velocity vectors generally decrease with time at a single location (Figure 4a-c) and generally the orientation of the velocity vectors becomes slightly more downvalley with time (Figure 4a-c). These observations are generally consistent with the evolution of the water table described earlier and presented in Figure 2a-e, but the orientation of the predicted velocity vectors in

Figure 4a - The near surface velocity field for day 30 (29 May 1996).

Figure 4b - The near surface velocity field for day 60 (29 June 1996).

Figure 4c - The near surface velocity field for day 90 (29 July 1996).

the central part of the study area is less downvalley that would be expected given the evolution of the piezometric surface (Figure 2a-e).

Velocity vectors are often high near the channel (Figure 4a-c). For the most part, these flows are toward the channel and have a vertical component which is downward which indicates that during this period, groundwater flow is into the stream. The pattern is consistent with a steep piezometric surface that develops particularly near elements 0 and 10 (Figure 2).

Accuracy of the results

We believe that the model itself works well producing accurate results given accurate input, as proved by the simulation of the Rushton and Redshow results. The factors affecting accuracy of the solution for the Banner Creek case are as follows:

(a) Theoretically sound boundary conditions are not available. The best we could do is to assume theoretical boundary conditions on the outskirts of the monitored region. For example, we assumed that head is constant (although different on each time step) across the vertical section on the boundaries since we knew head at only one point on the section. It is not quite so in reality. Usually, a condition like this is reasonable across a physical boundary (vertical or sloped) with a large reservoir.

(b) The precise material properties were not available. The most significant factor here is that the distribution of hydraulic conductivity is simply our best guess based on the data provided at some points and the observation of the pattern of water surface changes. For example, if at some points the drop in the water surface elevation is unusually high (as close to the region boundary along transects 2 and 3), we assumed the material to be of much higher conductivity there.

Data on the elastic properties (specific storage S_s) and the specific yield S_y were estimated as well.

(c) Theoretically sound initial conditions were not available. The data is constantly changing with time and there is no any moment in time when the distribution of head throughout the whole region--- not only on the boundaries--- is known. Any truly steady-state condition would be ideal since it would have made it possible to calculate head exactly at any point, and then base the further calculations on this data. We should point out, though, that such a lack of knowing a steady state prior to transient motion in practice happens very rarely. Alternatively, head can be measured in a great detail across the region in both horizontal and vertical directions. In our case, we just had to assume some initial state to be steady-state and calculate the initial head distribution based on this assumption. Inevitably, we introduce some error which then gets propagated through all calculations, resulting in a somewhat wiggling pattern of solution on successive time steps.

The situation can be demonstrated by this simplified example. Let some quantity be represented as $Q=f(x) - Q_o$, where f is some function and Q_o is the value of Q on the previous step. If

Q_o has been overestimated, then Q will be underestimated. That means, that on the next iteration Q_o (our previous Q) is underestimated and the new Q will be overestimated. This wiggling around the "true" solution continues unless somehow artificially removed.

(d) A theoretically sound estimate of the depth of the region is not known. We assumed the region's bottom to be at an elevation of 1520 m (4990 feet) and to be impervious.

Additional work and suggestions

Additional efforts appear necessary to improve model predictions of groundwater flow fields. As indicated above in the section on the accuracy of results, we believe these efforts must focus on better specification of input conditions - boundary conditions at the margin of the study area, better characterization of hydraulic conductivity over the region and with depth, and characterization of the specific storage (S_s) and the specific yield (S_y).

CONCLUSION

The three-dimensional version of the flow system model we developed (WaTab3D) was used to simulate groundwater flow in a portion of the valley bottom at Banner Creek, Idaho. The model predicts flow from the areas of highest elevation on the eastern edge and northeastern corner of the study area toward the channel on the western edge of the study area. In general, the vertical component of flow is downward over most of the study area. Velocity vectors generally decrease with time at a location. Near the channel, velocity vectors are locally large, toward the stream and typically downward indicating that the valley bottom is contributing water to the channel. Predicted flow is consistent in general with the observed piezometric surface and its evolution. Greater confidence in the results would require additional characterization of the hydraulic conductivity and boundary conditions within the study area.

REFERENCES CITED

Anderson, M.P., and W.W. Woessner, 1992, Applied groundwater modeling. Simulation of flow and advective transport; Academic Press, 382 pp.

Bear, J., 1972, Dynamics of fluids in porous media; Elsevier, N.Y., 764 pp.

Bencala, K.E., 1993, A perspective on stream-catchment connections; J. N. Am. Benthol. Soc., v. 12(1), p. 44-47.

De Wiest, R., J., M., Geohydrology, 368 pp., Wiley, 1965.

Freeze, R.A., and Cherry, J.A., 1979, Groundwater; Prentice-Hall; 606 pp.

Green, D.M., and J.B. Kauffman, 1989, Nutrient cycling at the land-water interface - the importance of the riparian zone. In: Practical approaches to riparian resource management, R.E. Gresswell, B.A. Barton, and J.L. Kershner (eds.), USDI Bureau of Land Management, Billings, MT, p. 61-68

Kazda, I., 1990, Finite element techniques in groundwater flow studies: with applications in hydraulic and geotechnical engineering; Elsevier, 314 pp.

Kondolf, G.M., L.M. Maloney, and J.G. Williams, 1987, Effects of bank storage and well pumping on baseflow, Carmel River, Monterrey County, California; Journal of Hydrology, v. 91, p. 351-369

Moss, E.H., 1938, Longevity of seed and establishment of seedlings in species of Populus: Botanical Gazette, v. 99, p. 529-542.

National Research Council, 1991, Opportunities in the Hydrologic Sciences; National Academy Press, 348 pp.

Neuman, S.P., 1976, User's guide for FREESURF I; Dept. Hydrology and Water Resources, Univ. of Arizona, Tucson, Arizona, 22 pp.

Neuman, S.P., and P.A. Witherspoon, 1970a, Finite element method of analyzing steady seepage with a free surface, Water Resour. Res., v. 6(3), p. 889-897.

Neuman, S.P., and P.A. Witherspoon, 1970b, Variational principles for confined and unconfined flow of groundwater; Water Resour. Res., v. 6(5), p. 1376-1382.

Neuman, S.P., and P.A. Witherspoon, 1971, Analyzing of nonsteady flow with a free surface using the finite element method; Water Resour. Res., v. 7(3), p. 611-623.

Oregon State University Water Resources Institute, 1986, Estimating and measuring impacts of non-structural methods for increasing basin water yield; Report to the 3rd Interuniversity Water workshop, Portland State University, Portland, OR, May 9, 1986, 47 pp.

Peterjohn, W.T., and D.L. Correll, 1984, Nutrient dynamics in an agricultural watershed: observations on the role of a riparian forest; Ecology, v. 65, p. 1466-1475.

Polubarinova-Kochina, P.Y., 1962, The theory of groundwater movement; Princeton University Press, Princeton, J, 613 pp.

Ponce, V.M., 1989, Baseflow augmentation by streambank storage; Report prepared for Pacific Gas and Electric, October, 1989, 91 pp.

Rushton, K.R., and S.C. Redshaw, 1979, Seepage and groundwater flow; Wiley, 340 pp.

Whiting, P.J., and M. Pomeranets, 1997, A numerical study of bank storage and its contribution to streamflow, Journal of Hydrology, v. 202, p. 121-136.

Wilson, R.E., 1970, Succession in stands of *Populus deltoides* along the Missouri River in southeastern South Dakota; American Midland Naturalist, v. 83, p. 330-342.

Winegar, H.H., 1977, Camp Creek channel fencing - plant, wildlife, soil and water response; Rangeman's Journal, v. 4(1), p. 10-12.

APPENDIX A -

EVOLUTION OF THE FLOW FIELD

15 days after start (5/14/96); layer 0

[new data]

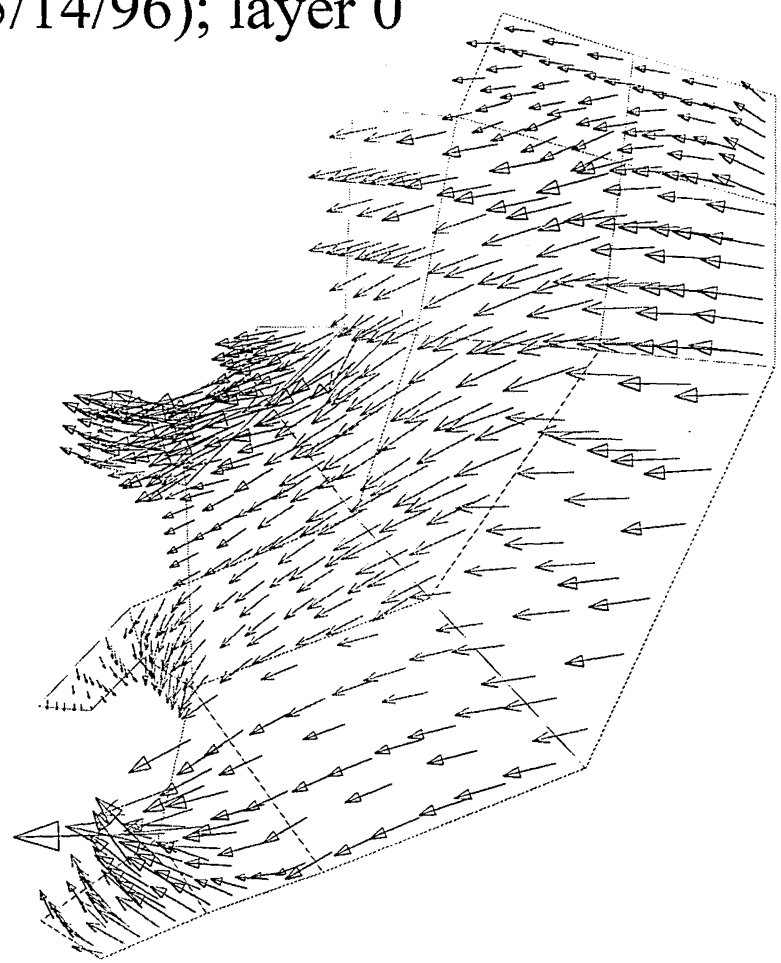

is 26.3842

15 days after start (5/14/96); layer 1 [new data]

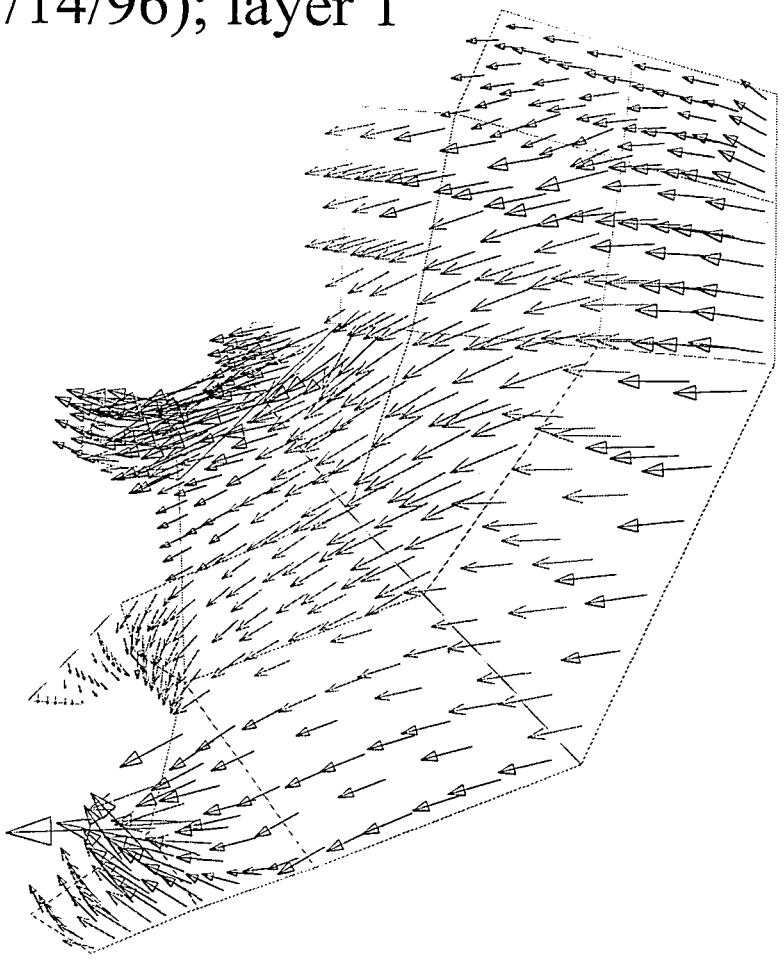

is 26.3842

15 days after start (5/14/96); layer 2 [new data]

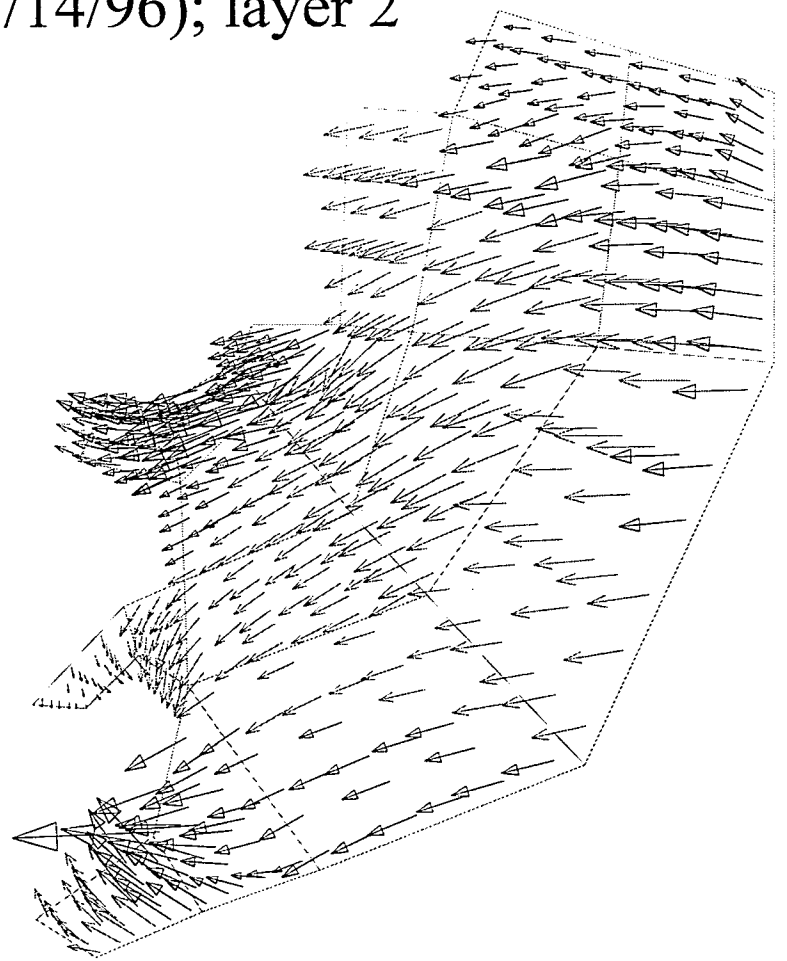

is 26.3842

15 days after start (5/14/96); layer 3 [new data]

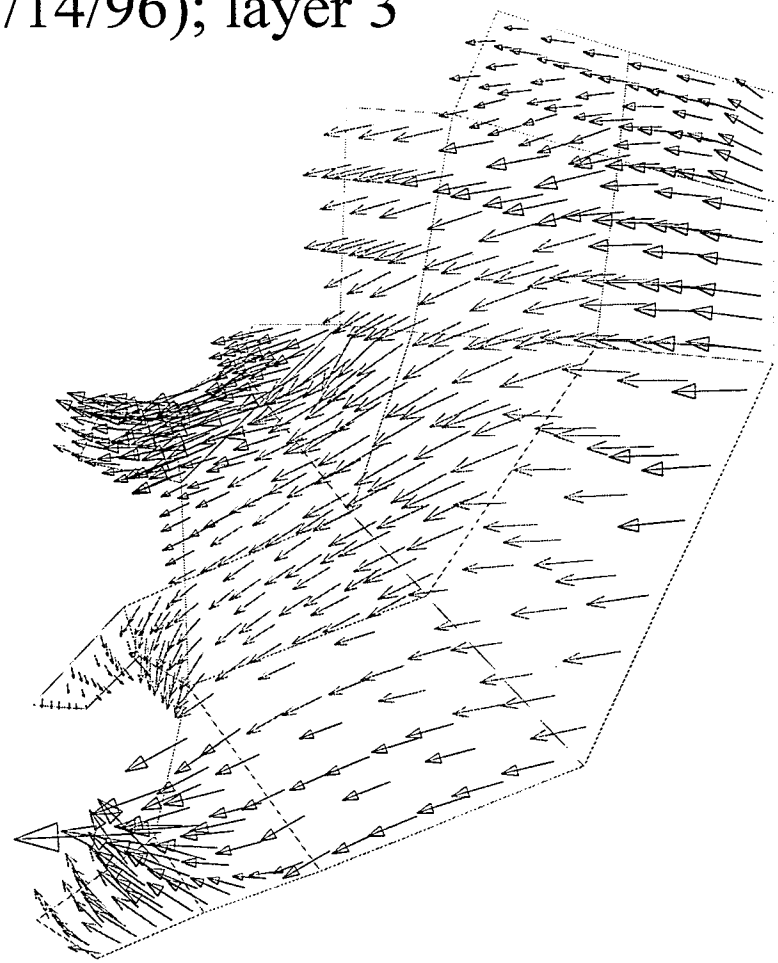

is 26.3842

15 days after start (5/14/96); layer 4 [new data]

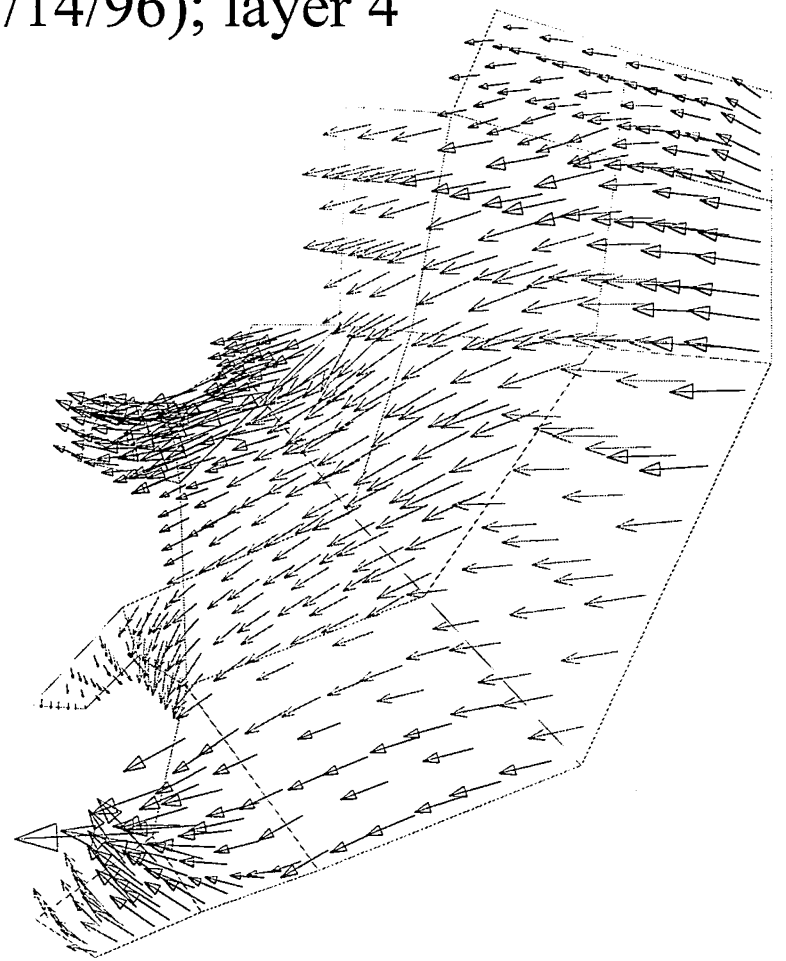

is 26.3842

15 days after start (5/14/96); layer 5 [new data]

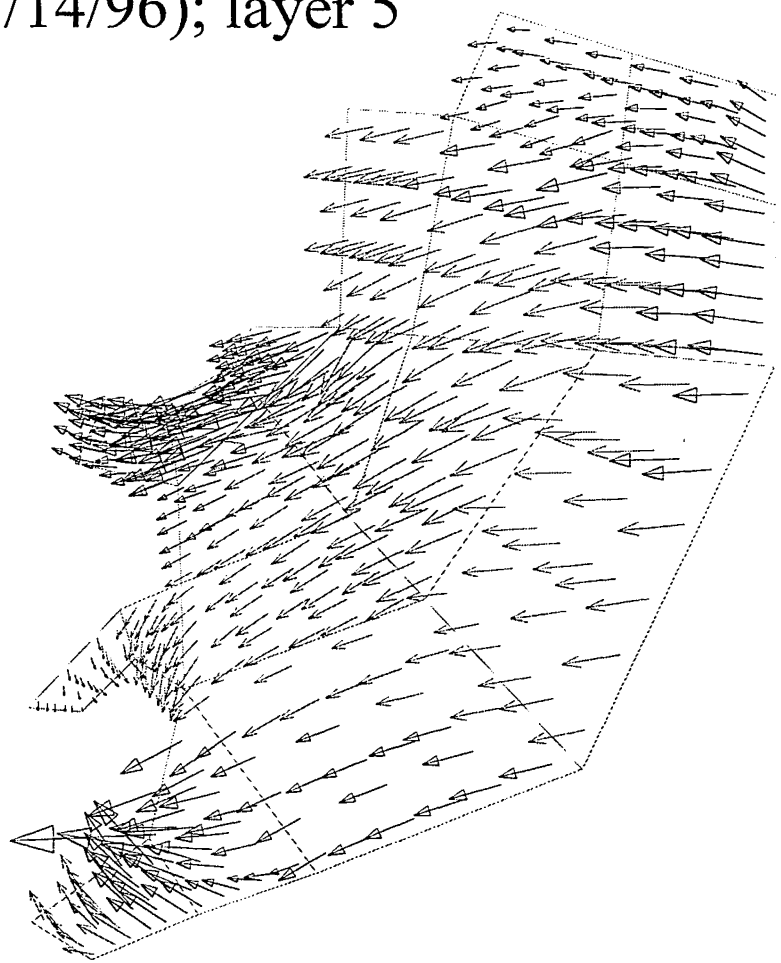

is 26.3842

30 days after start (5/29/96); layer 0 [new data]

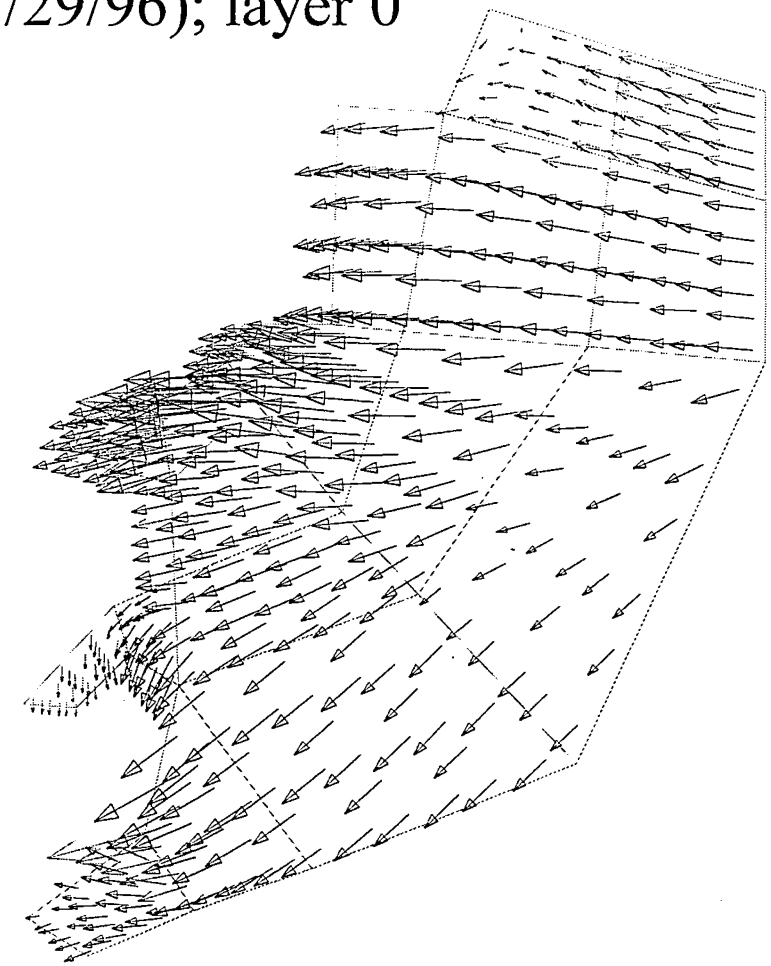

is 26.3842

30 days after start (5/29/96); layer 1 [new data]

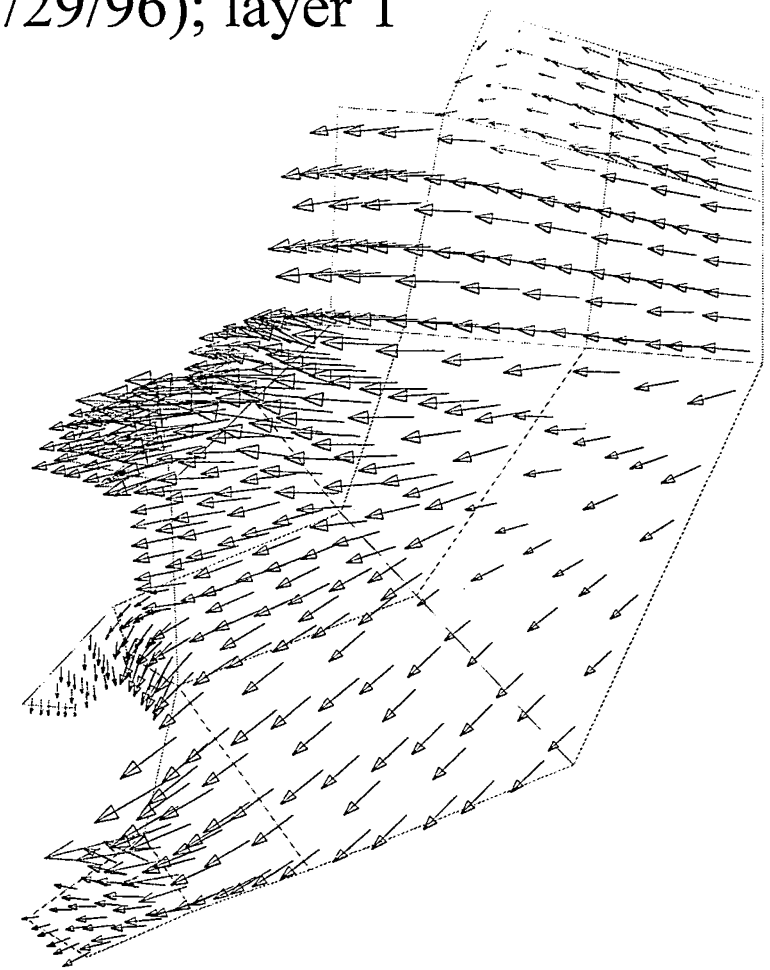

is 26.3842

30 days after start (5/29/96); layer 2 [new data]

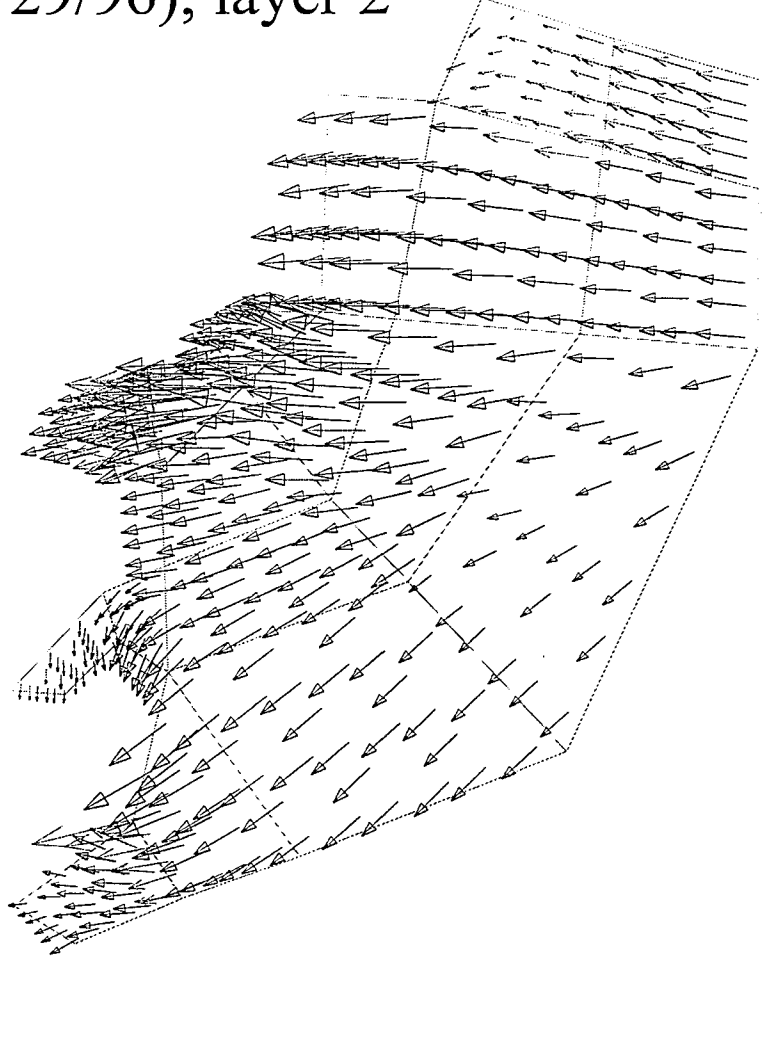

is 26.3842

30 days after start (5/29/96); layer 3 [new data]

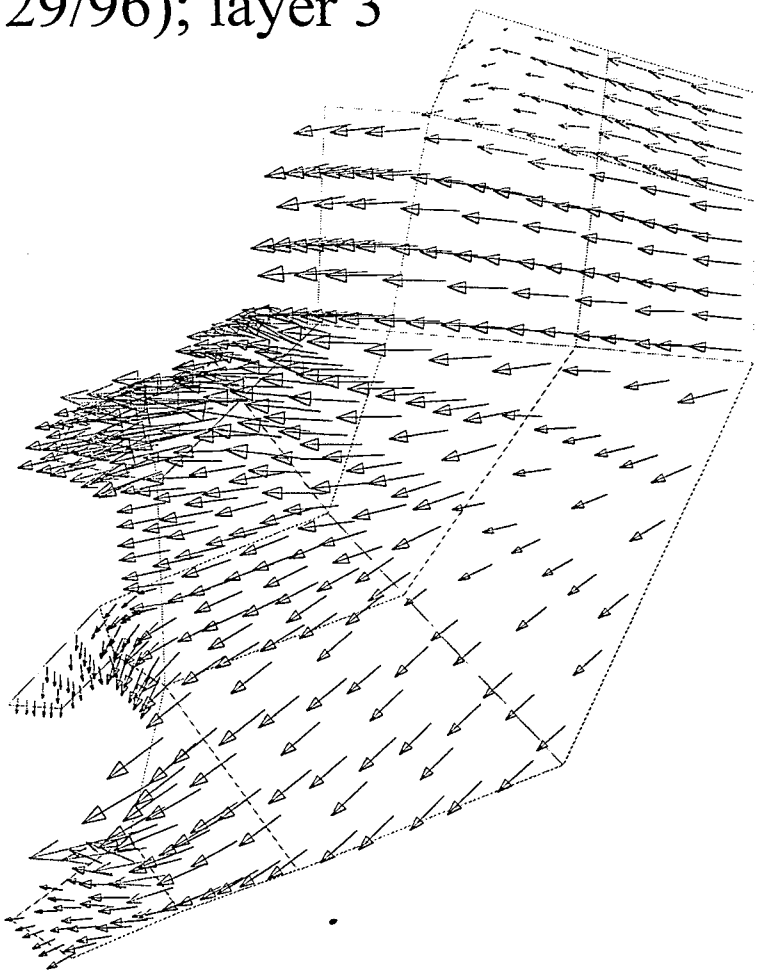

is 26.3842

30 days after start (5/29/96); layer 4 [new data]

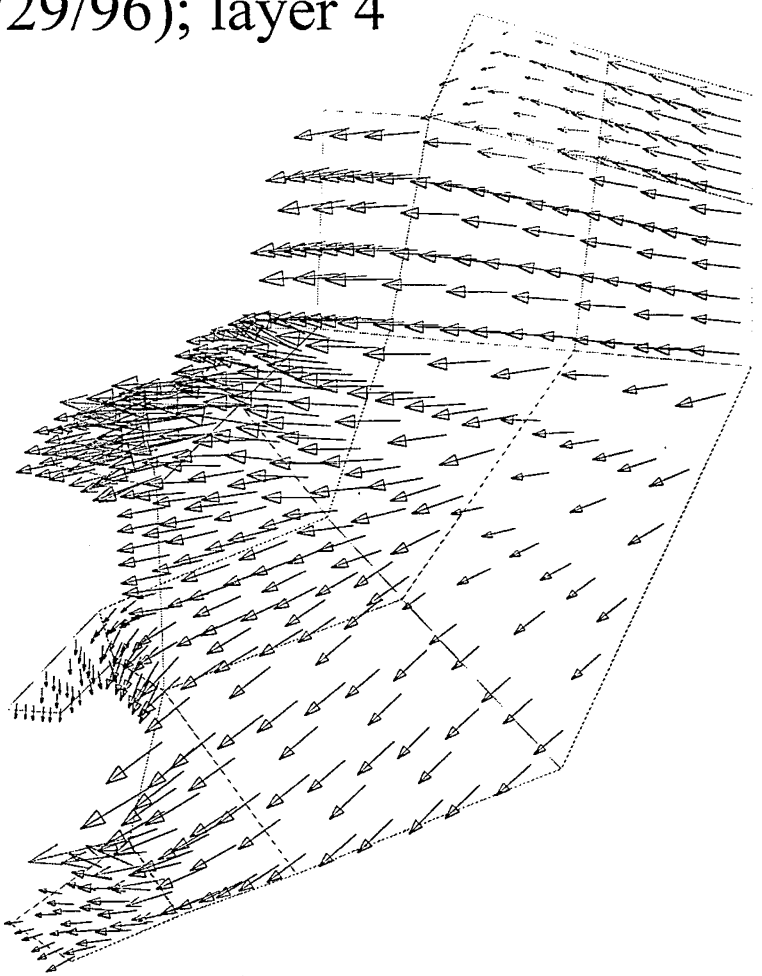

is 26.3842

30 days after start (5/29/96); layer 5 [new data]

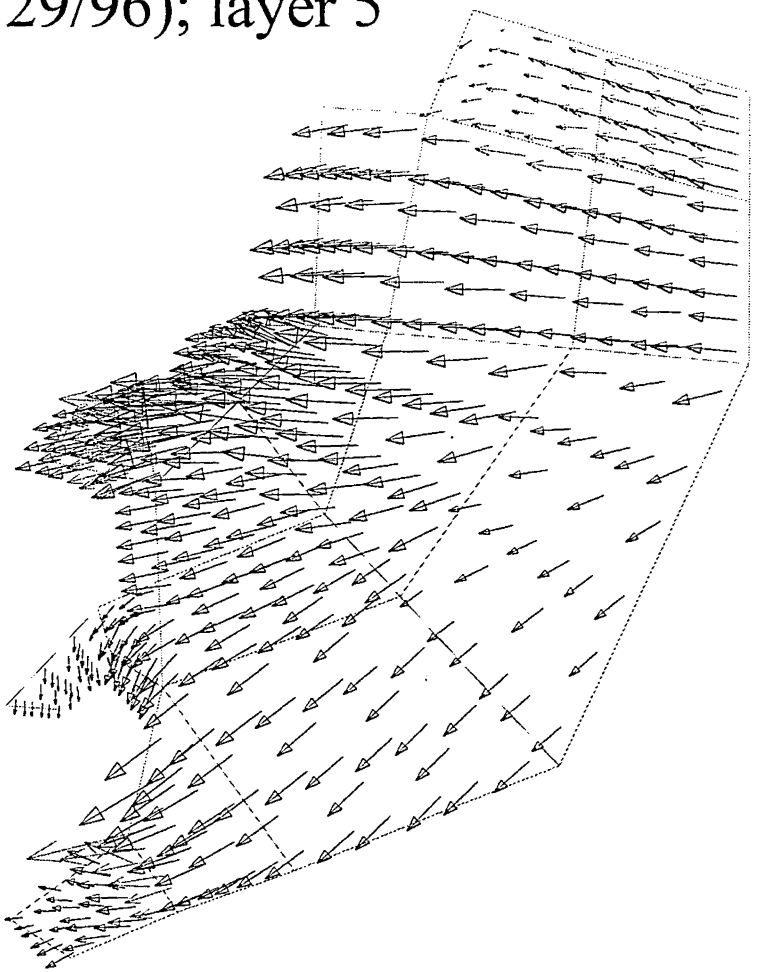

is 26.3842

45 days after start (6/14/96); layer 0 [new data]

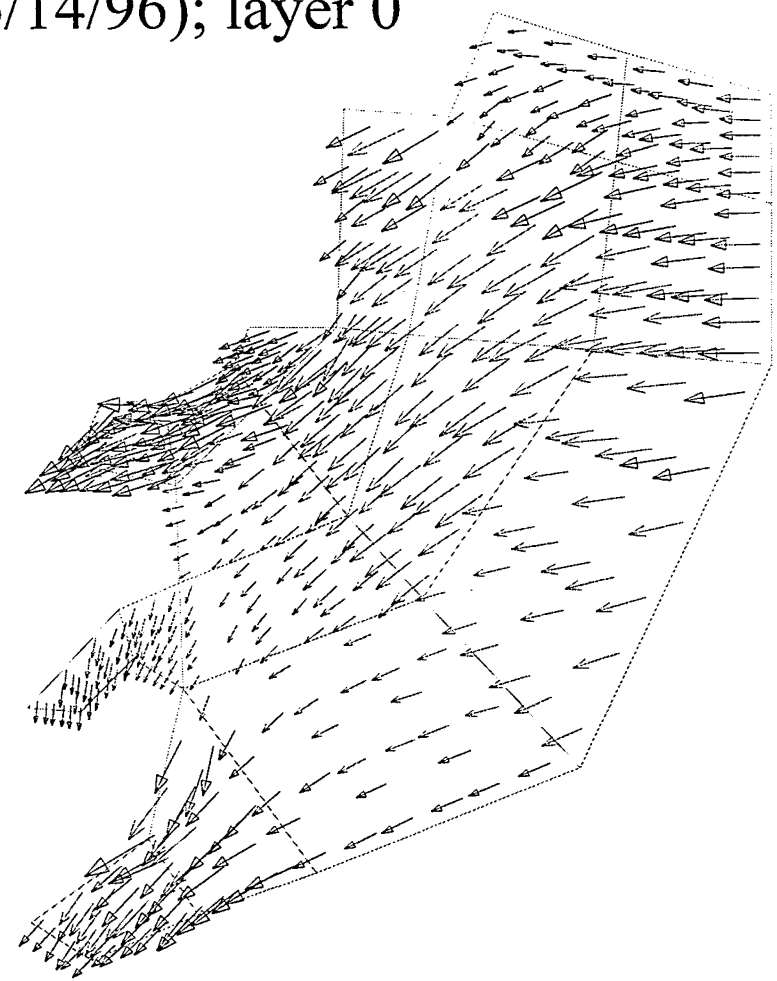

is 26.3842

45 days after start (6/14/96); layer 1 [new data]

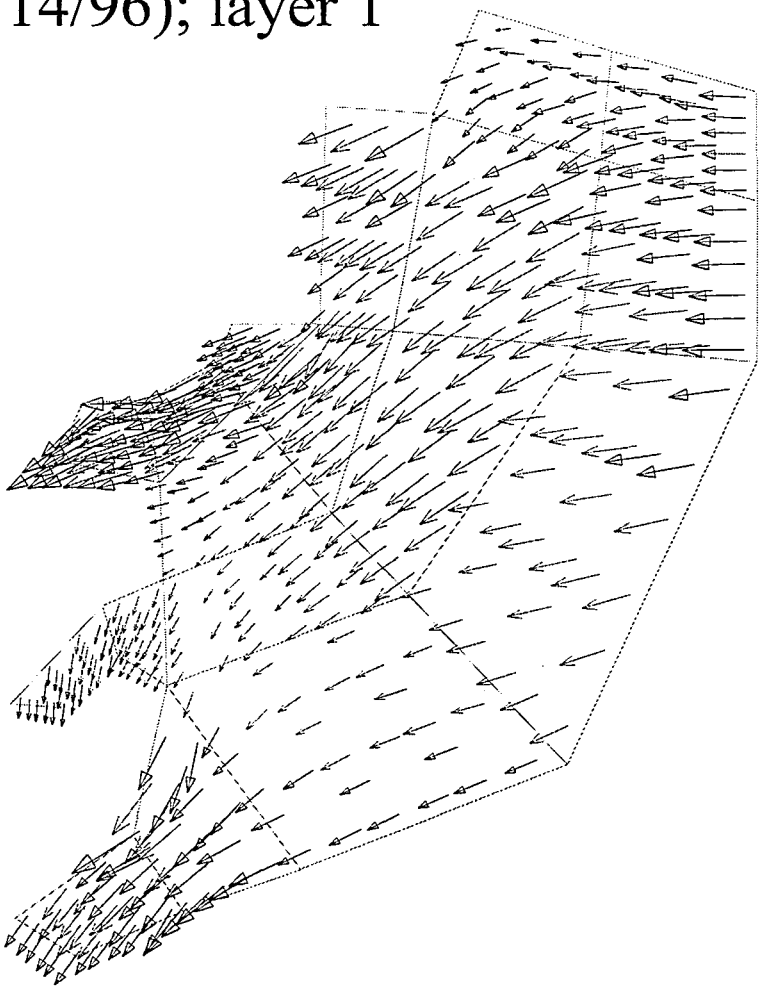

is 26.3842

45 days after start (6/14/96); layer 2 [new data]

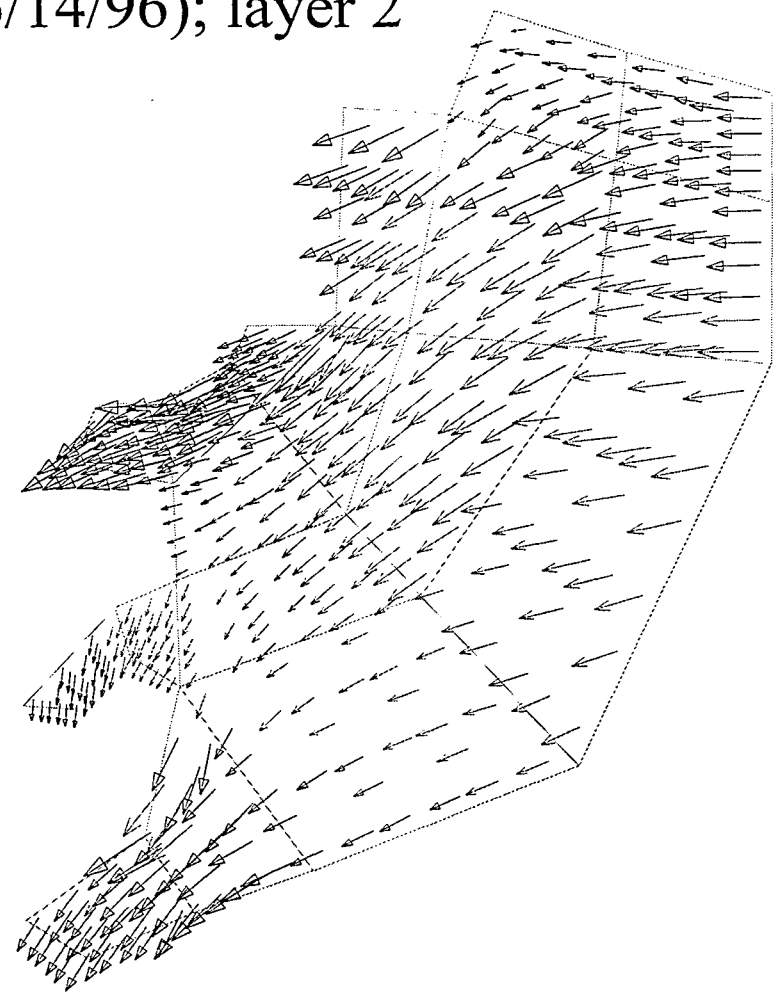

is 26.3842

45 days after start (6/14/96); layer 3 [new data]

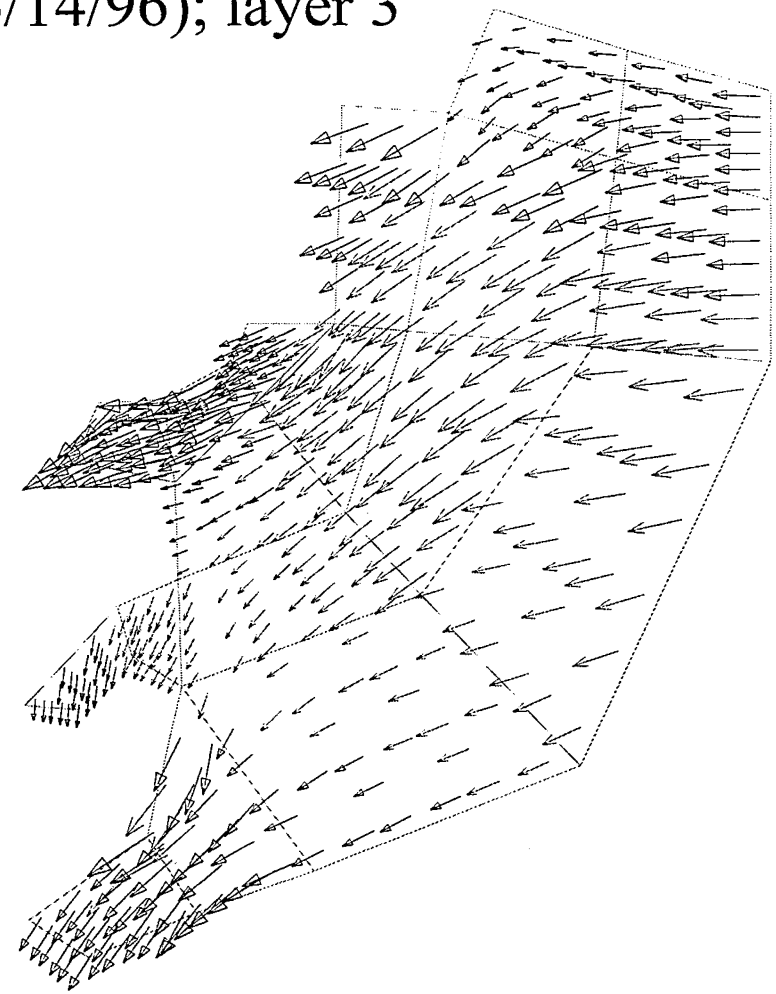

is 26.3842

45 days after start (6/14/96); layer 4

[new data]

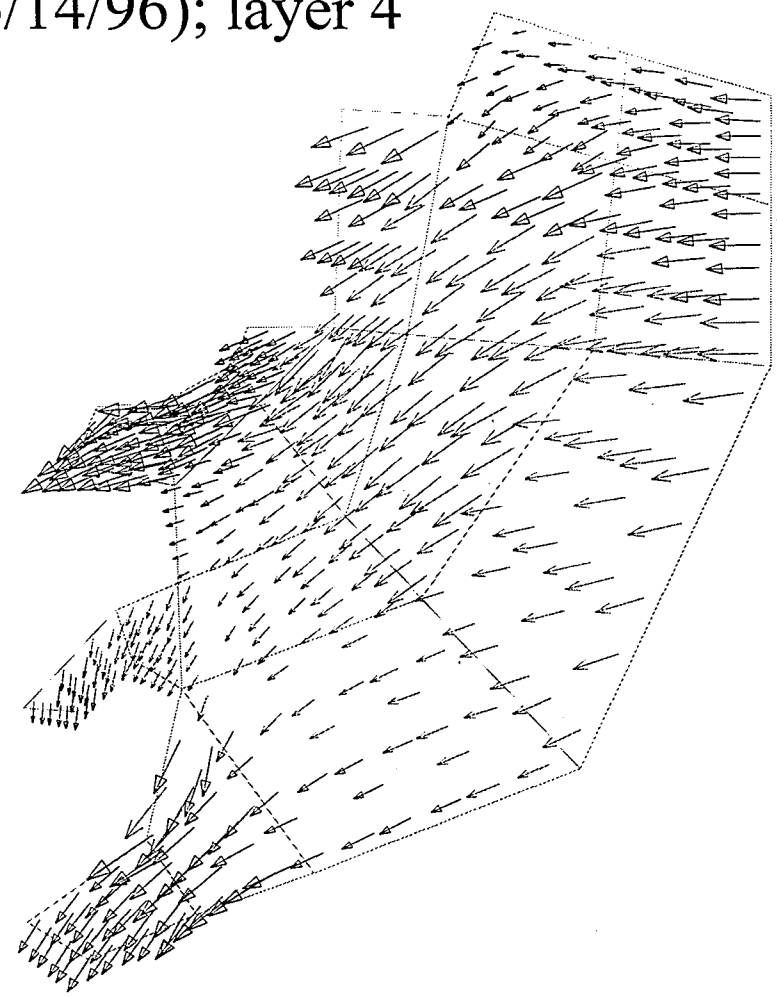

is 26.3842

45 days after start (6/14/96); layer 5 [new data]

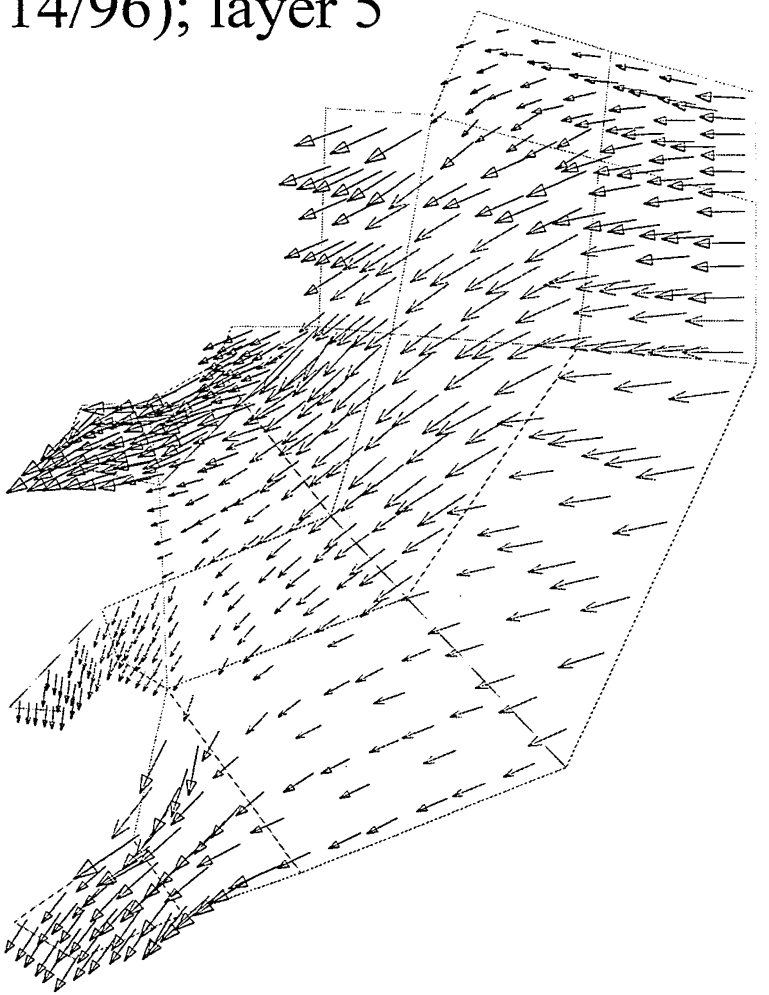

is 26.3842

60 days after start (6/29/96); layer 0 [new data]

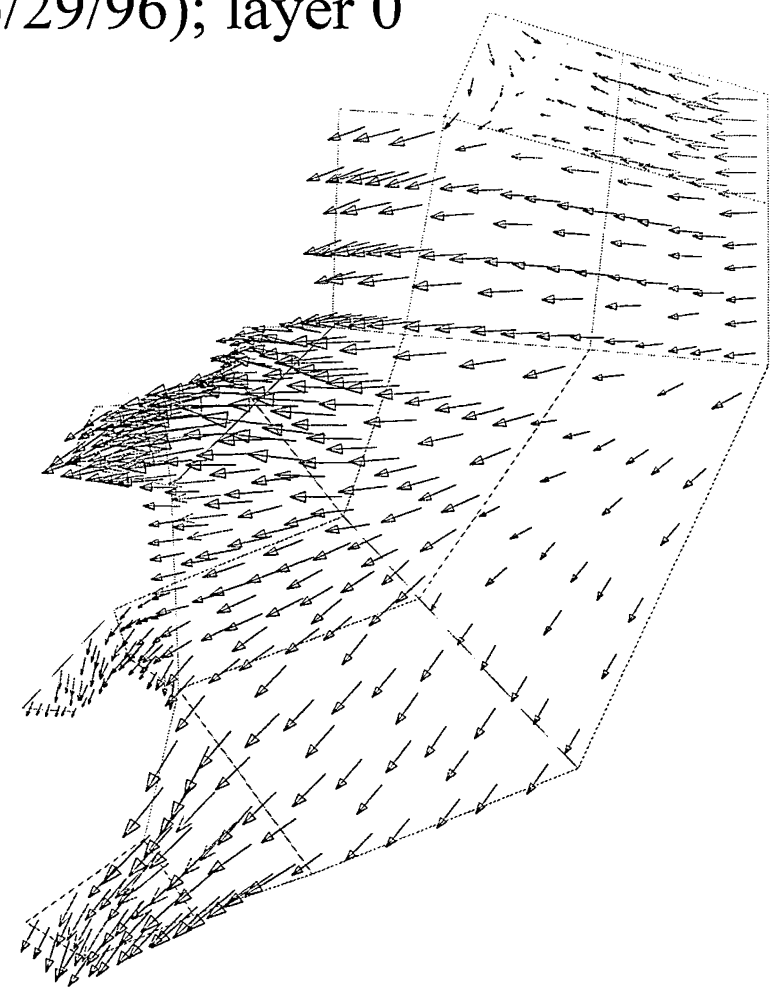

is 26.3842

60 days after start (6/29/96); layer 1 [new data]

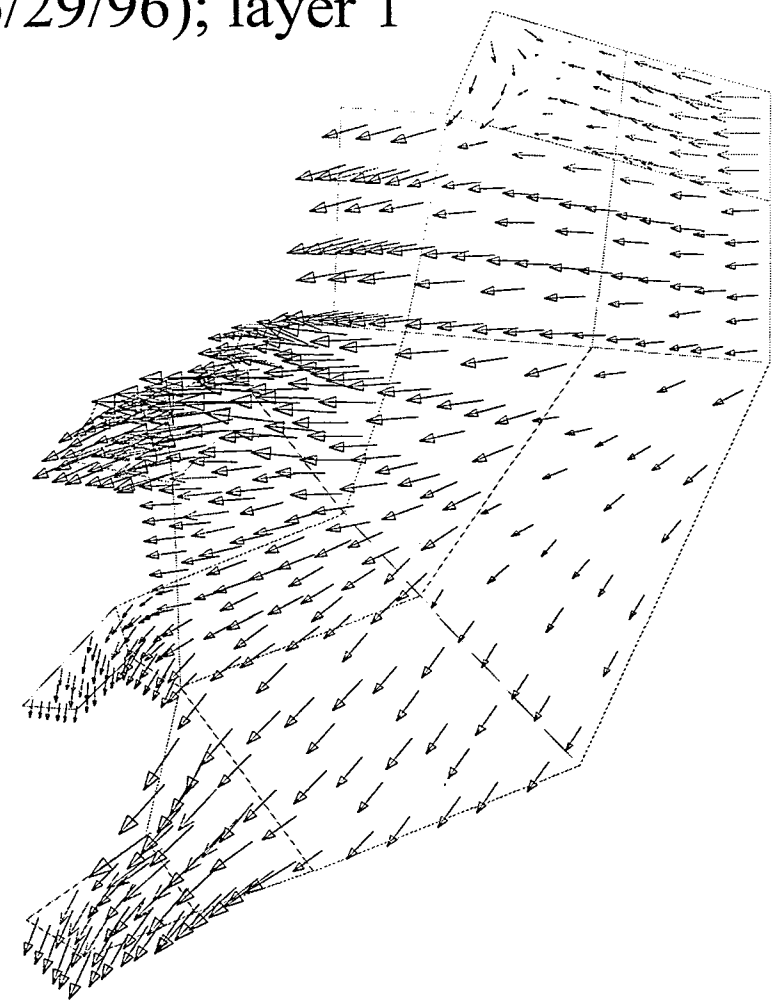

is 26.3842

60 days after start (6/29/96); layer 2 [new data]

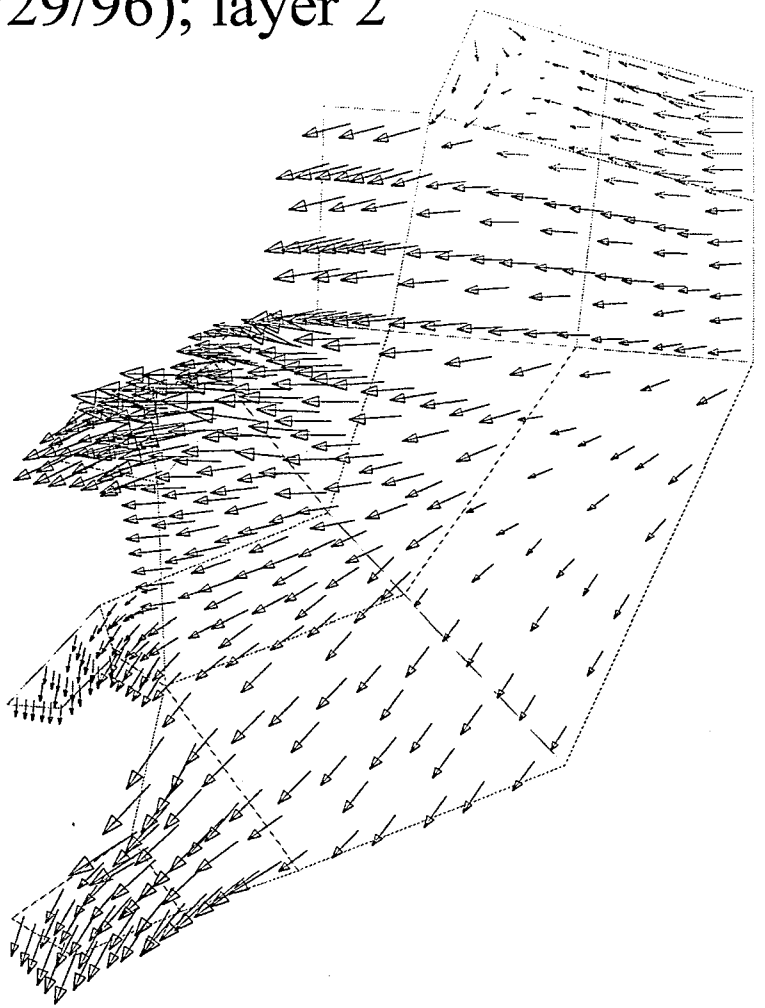

is 26.3842

60 days after start (6/29/96); layer 3 [new data]

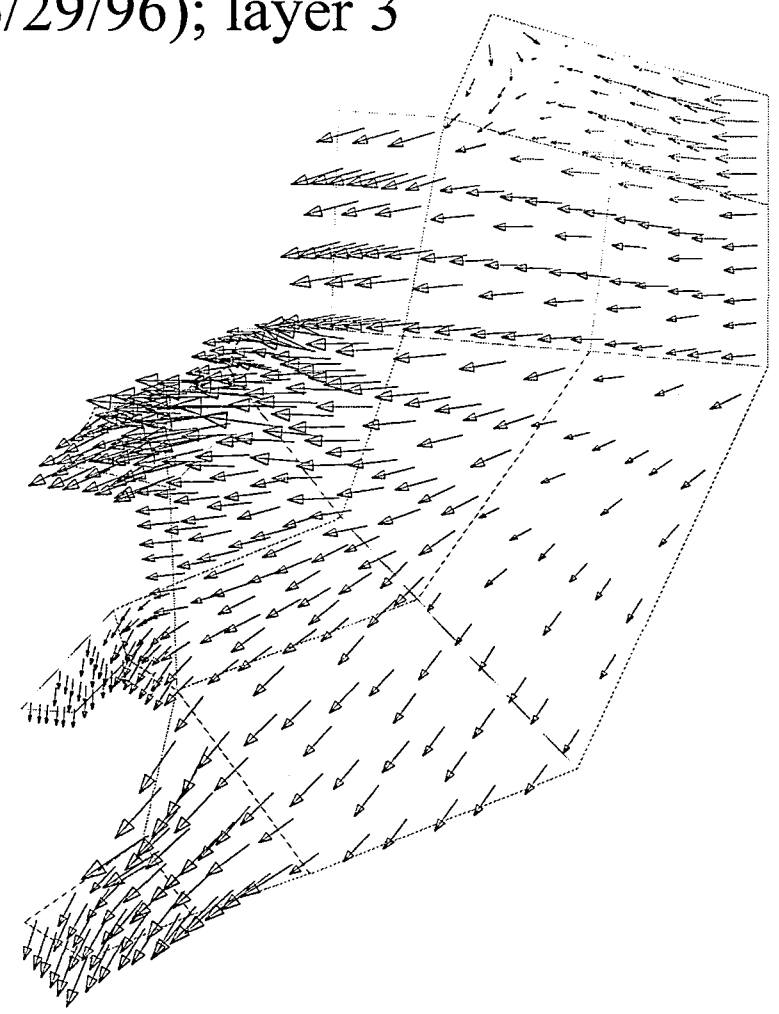

is 26.3842

60 days after start (6/29/96); layer 4 [new data]

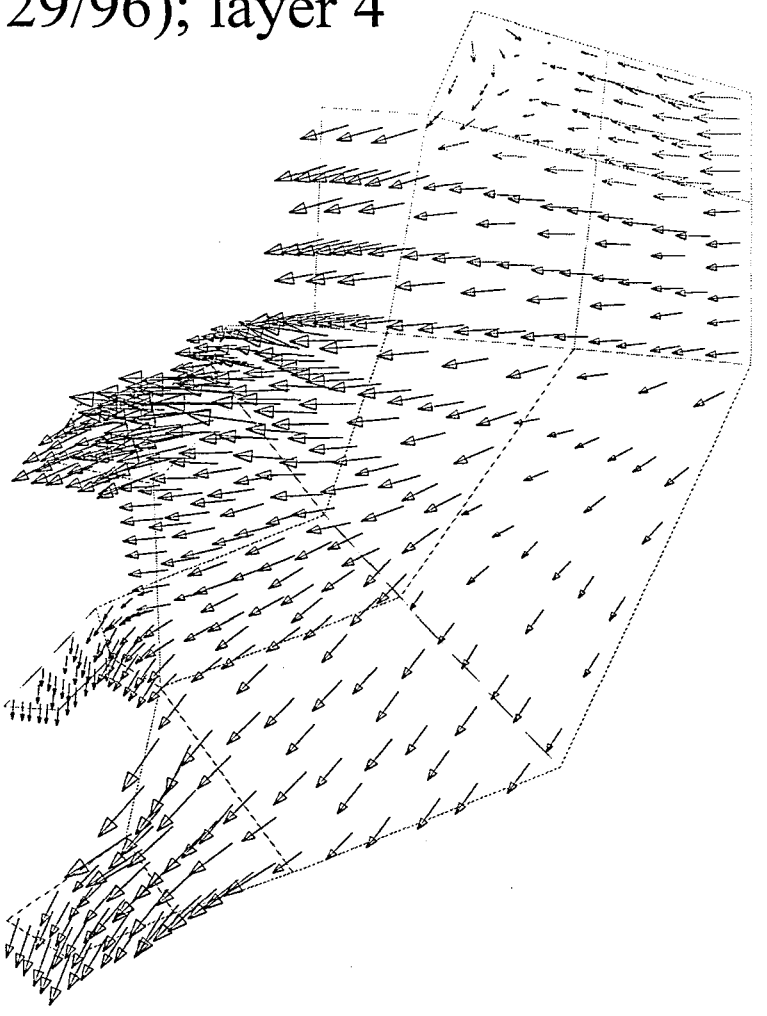

is 26.3842

60 days after start (6/29/96); layer 5 [new data]

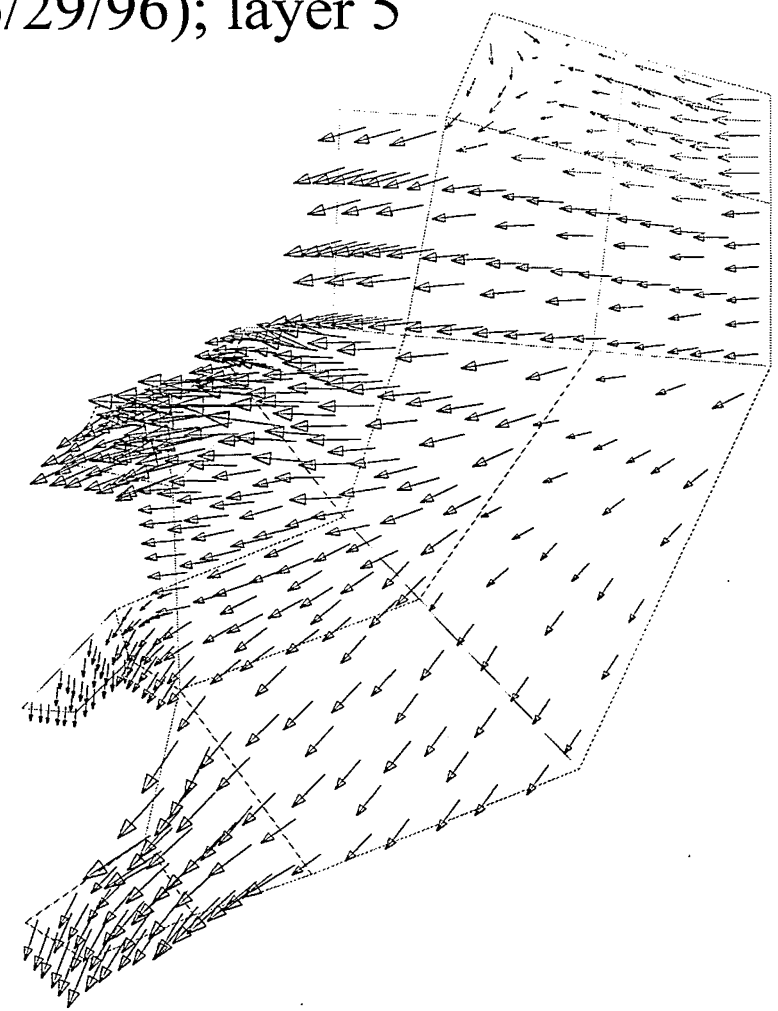

is 26.3842

75 days after start (7/14/96); layer 0 [new data]

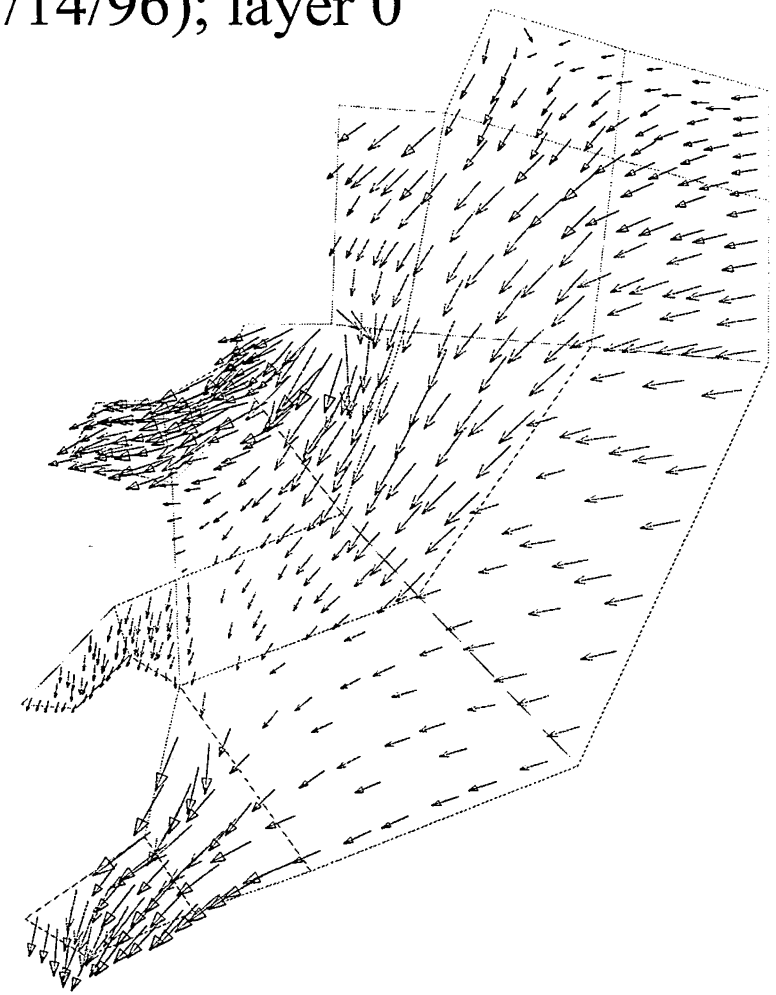

is 26.3842

75 days after start (7/14/96); layer 1 [new data]

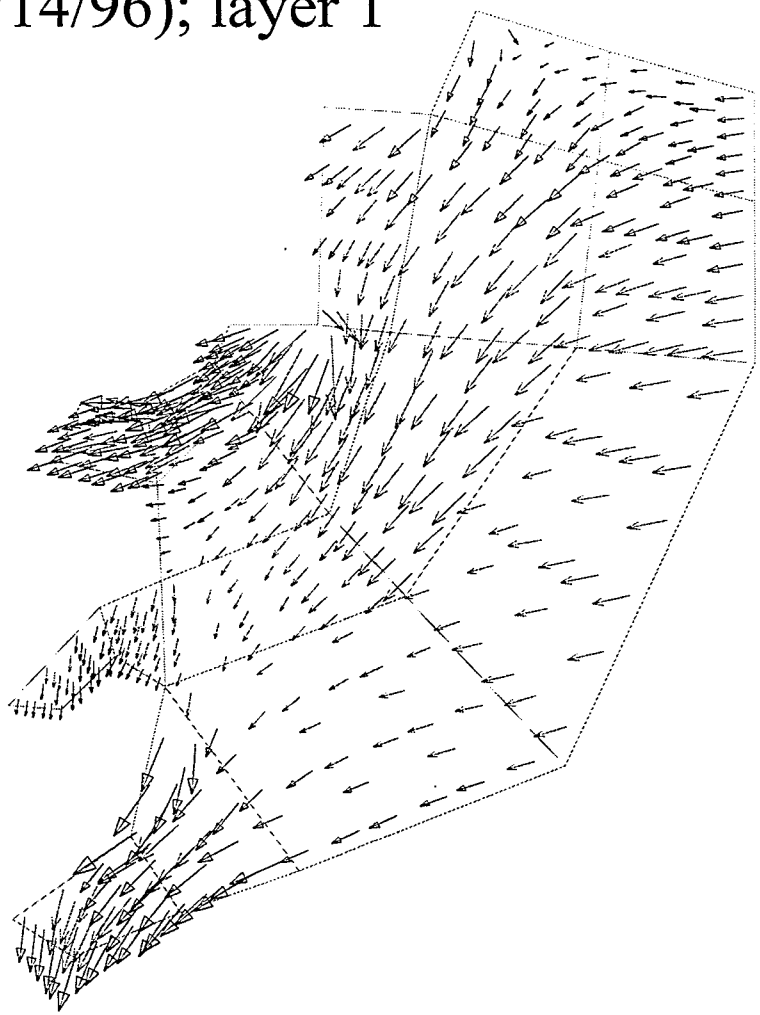

is 26.3842

75 days after start (7/14/96); layer 2 [new data]

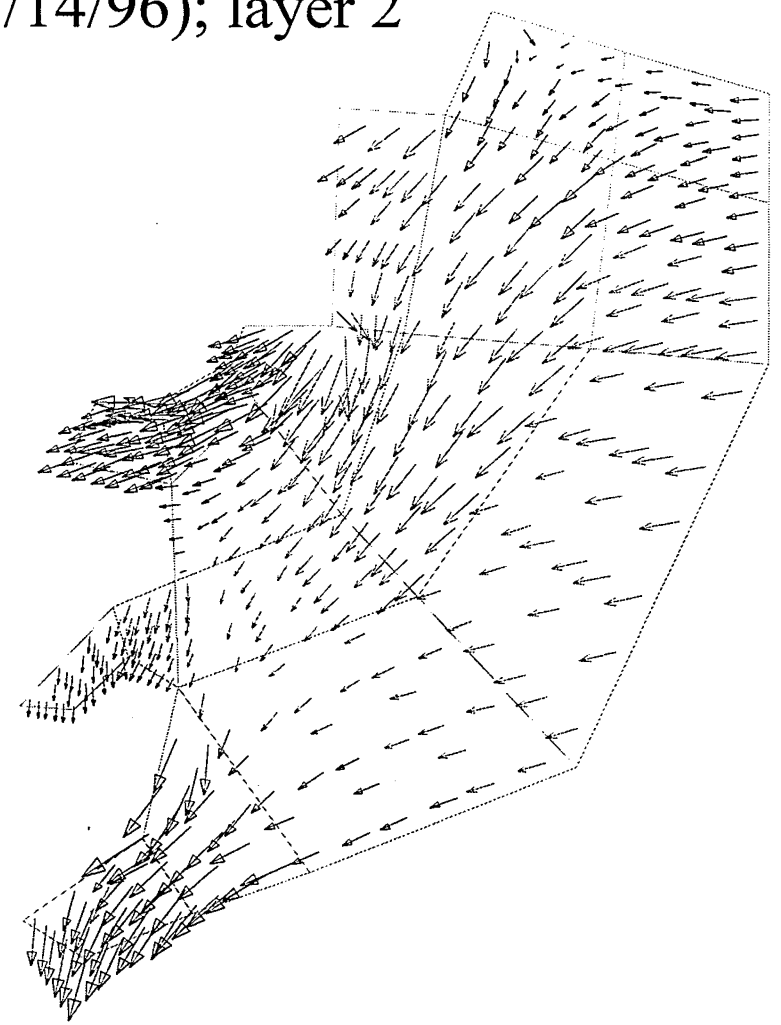

is 26.3842

75 days after start (7/14/96); layer 3 [new data]

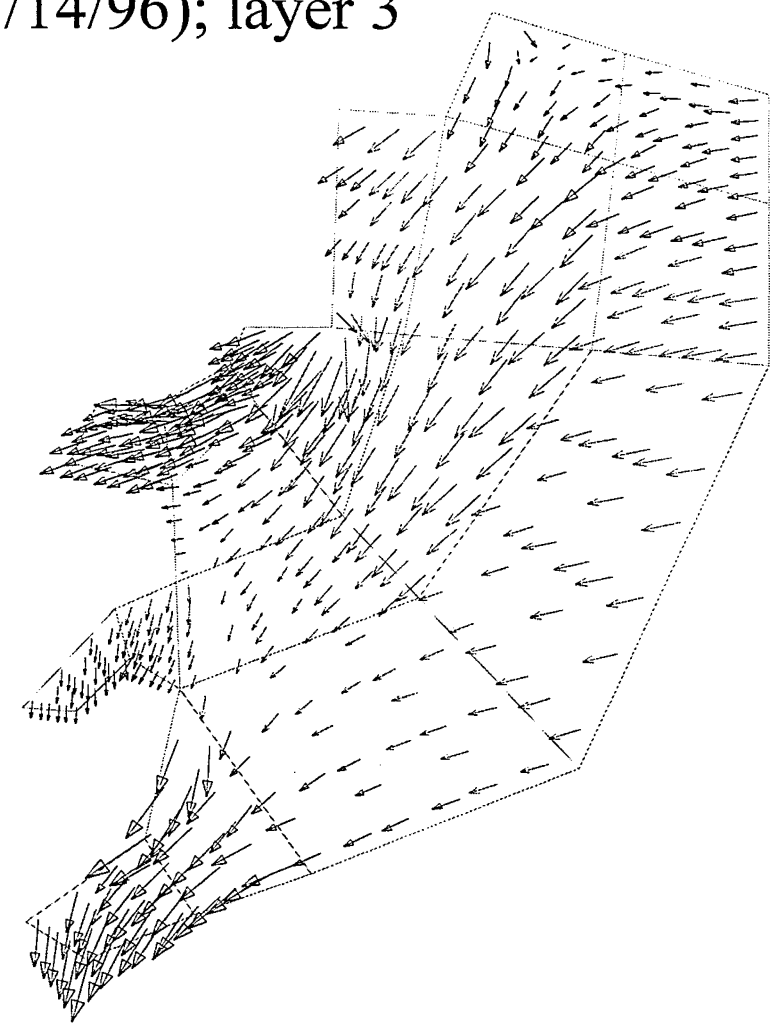

is 26.3842

75 days after start (7/14/96); layer 4 [new data]

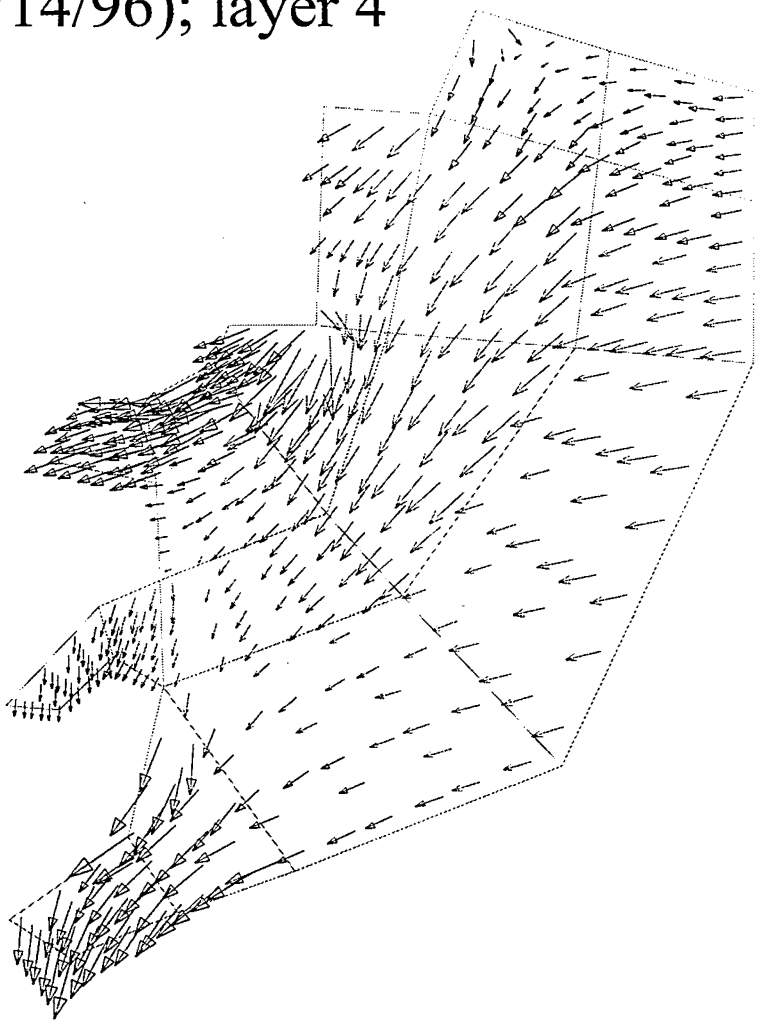

is 26.3842

75 days after start (7/14/96); layer 5 [new data]

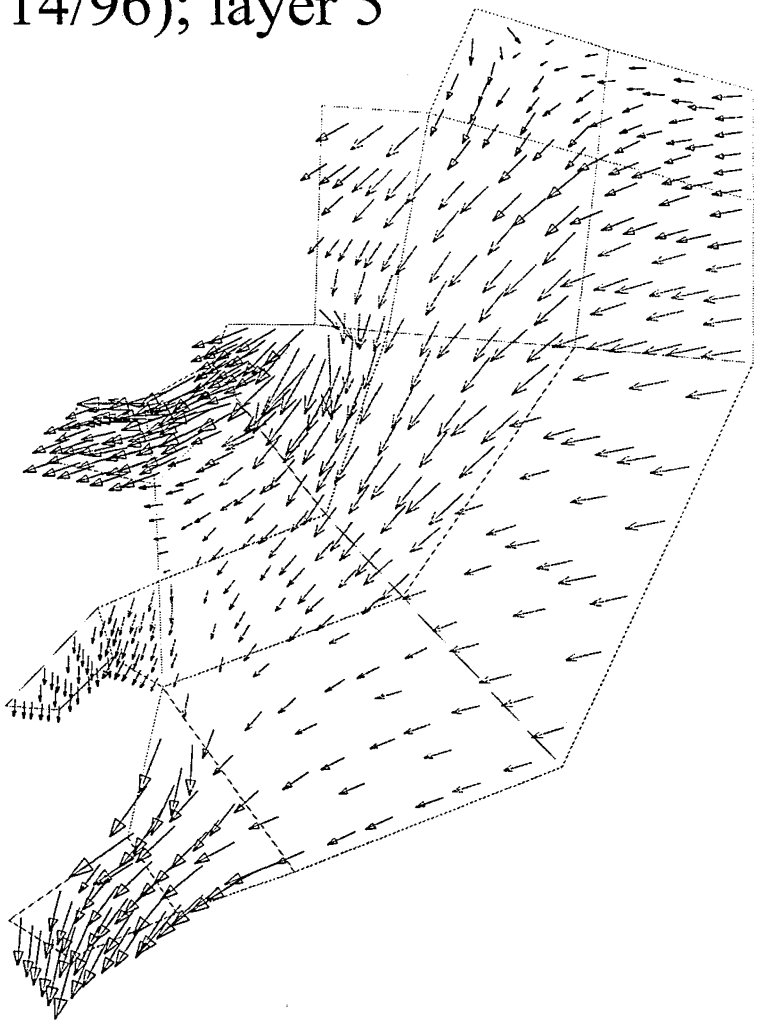

is 26.3842

90 days after start (7/29/96); layer 0 [new data]

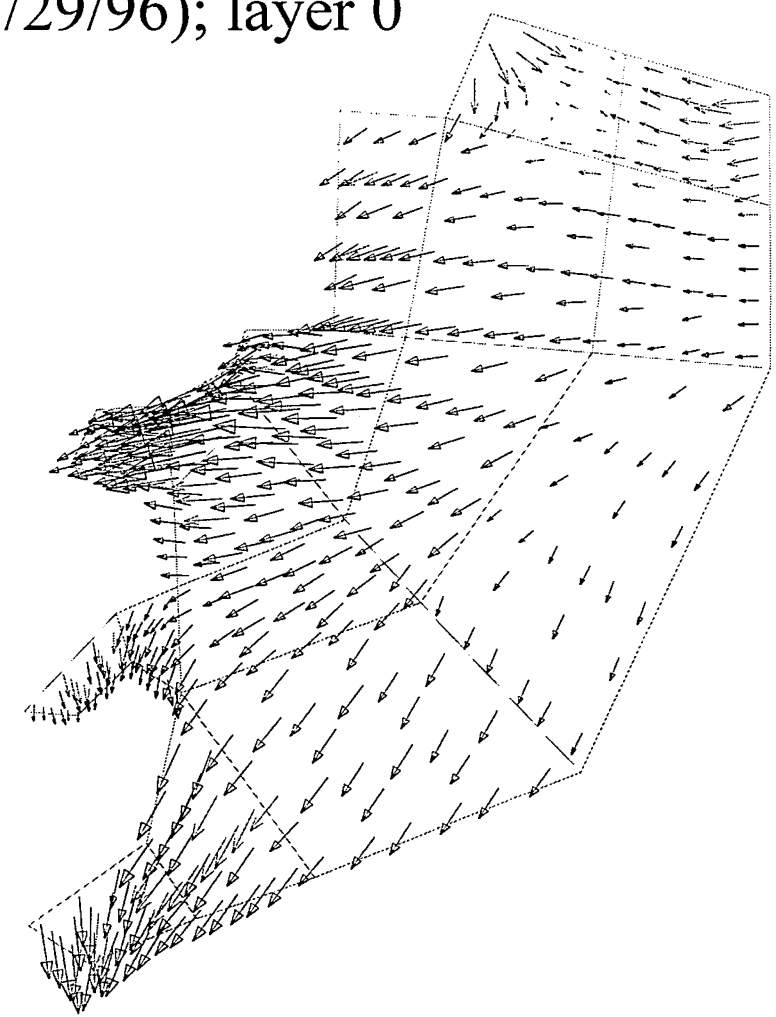

is 26.3842

90 days after start (7/29/96); layer 1 [new data]

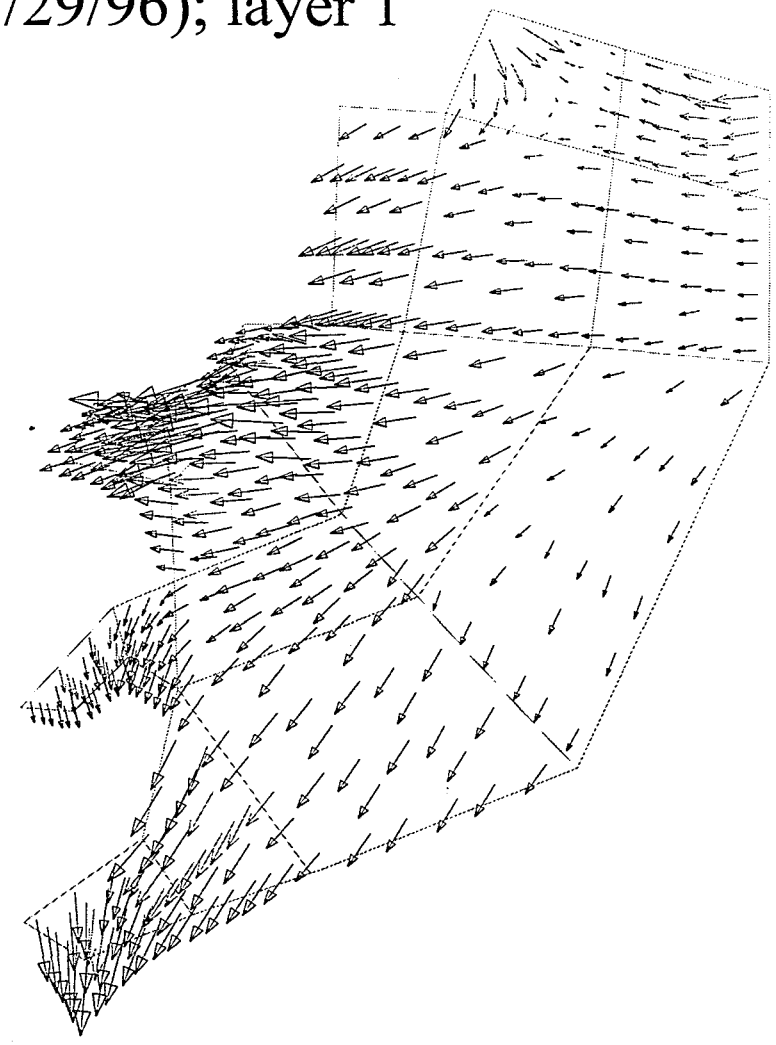

is 26.3842

90 days after start (7/29/96); layer 2 [new data]

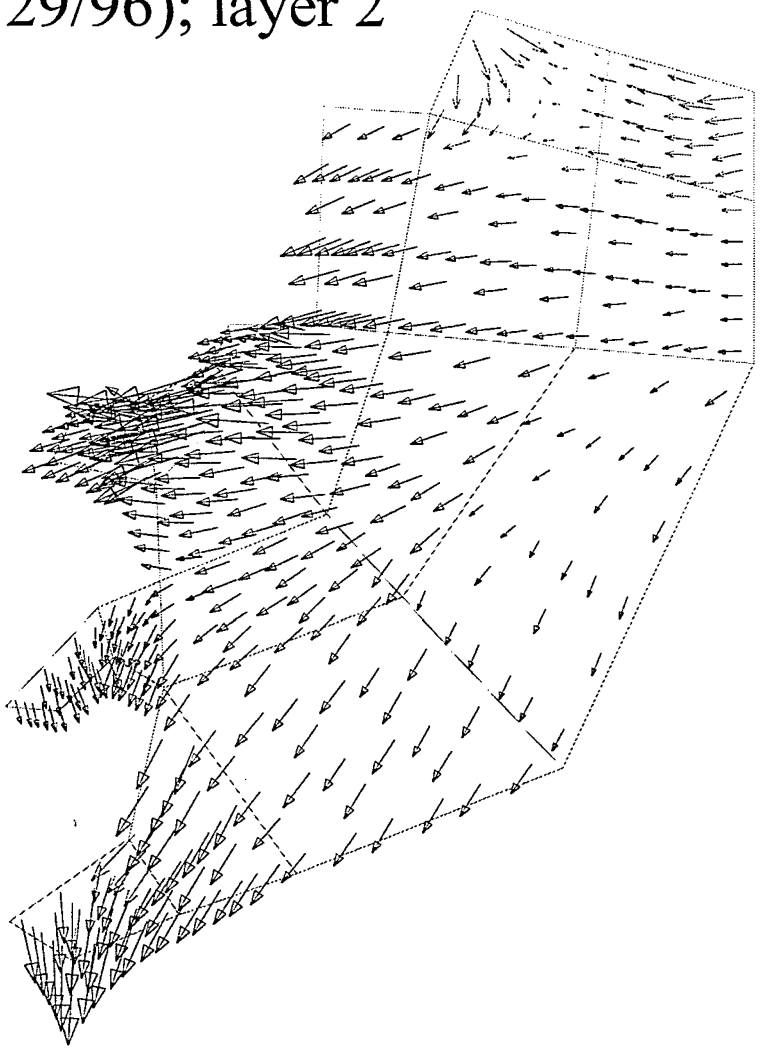

is 26.3842

90 days after start (7/29/96); layer 3 [new data]

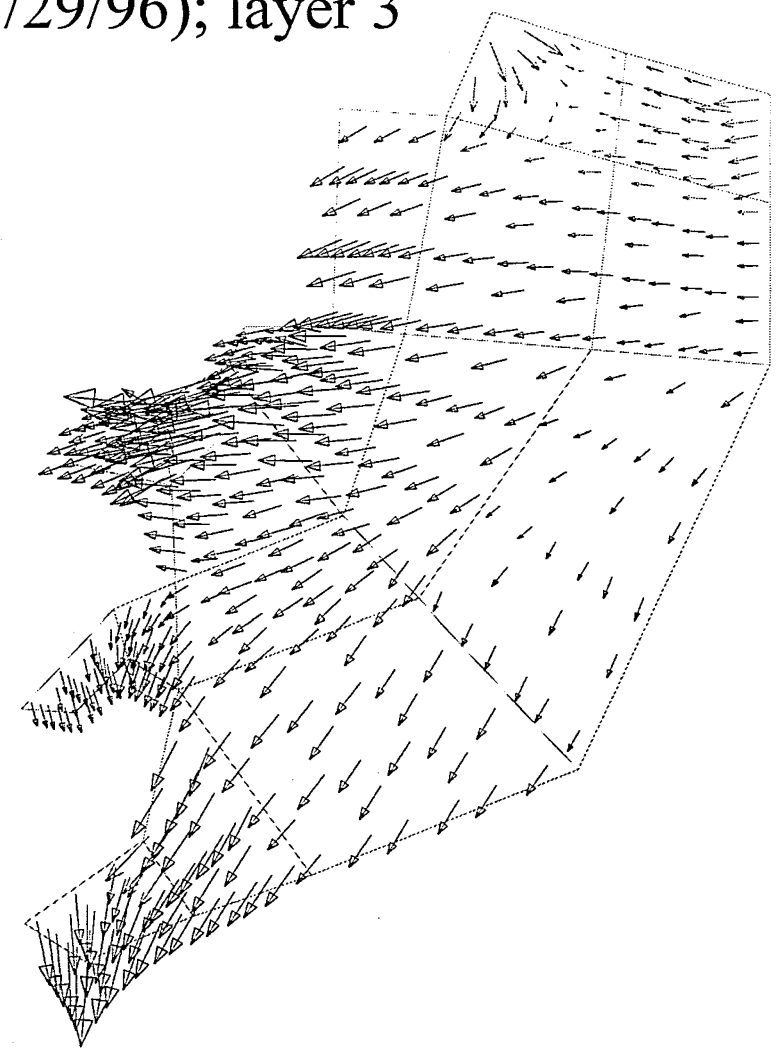

is 26.3842

90 days after start (7/29/96); layer 4 [new data]

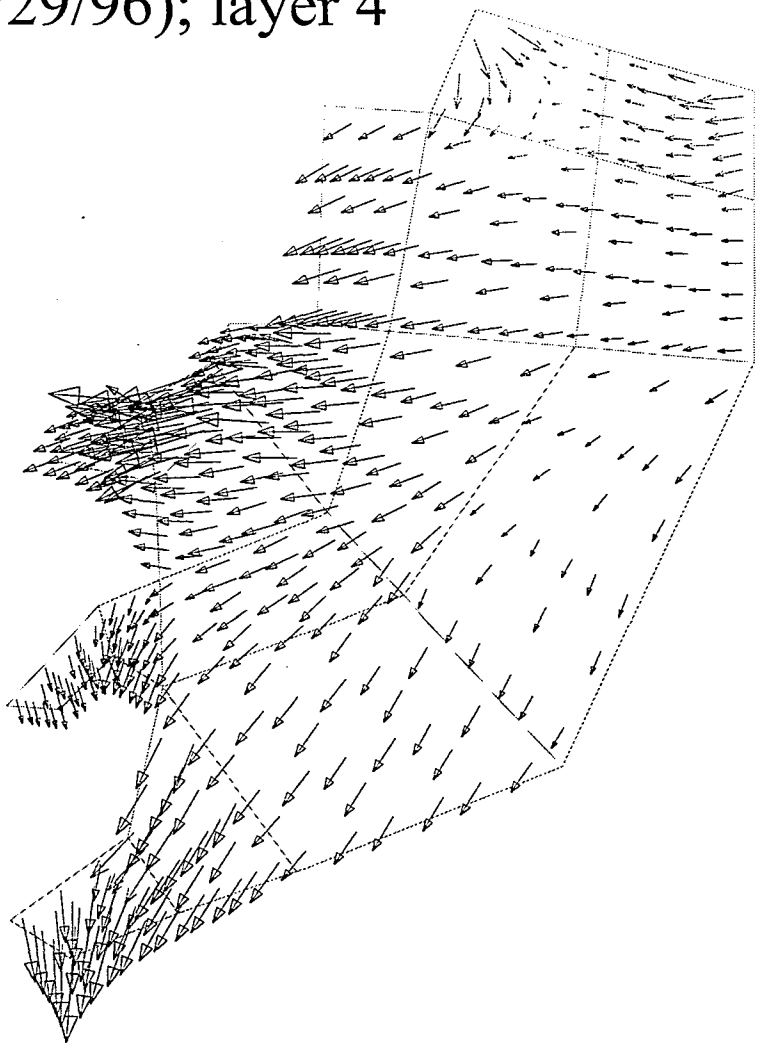

is 26.3842

90 days after start (7/29/96); layer 5 [new data]

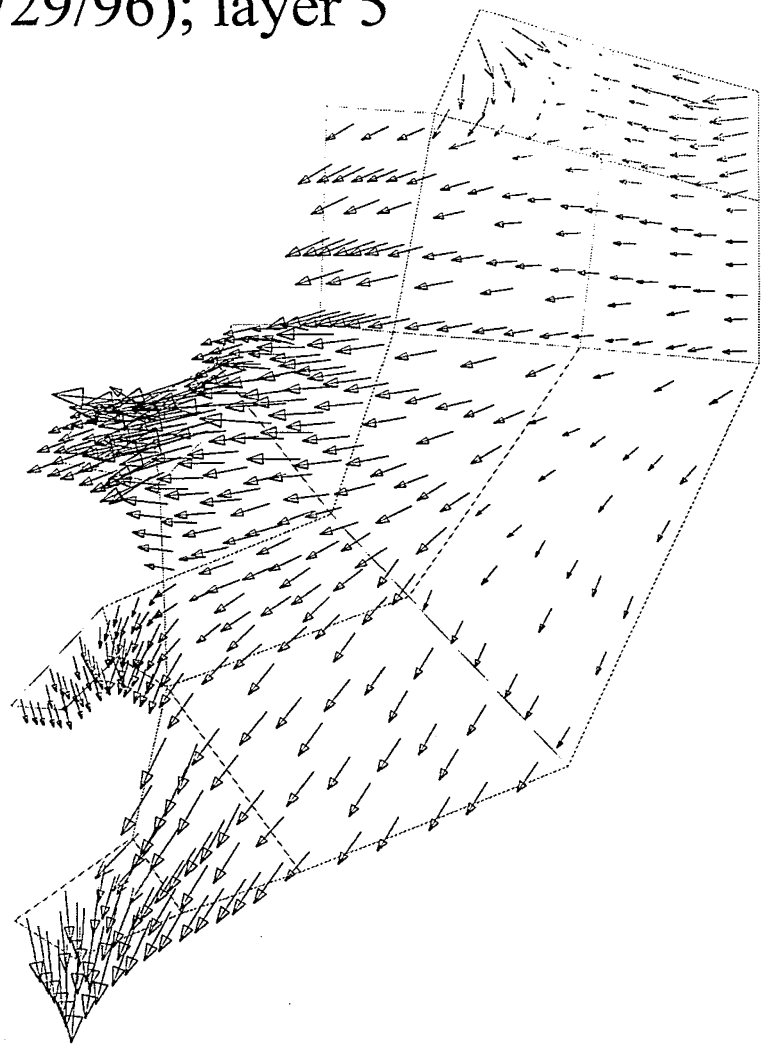

is 26.3842

105 days after start (8/14/96); layer 0 [new data]

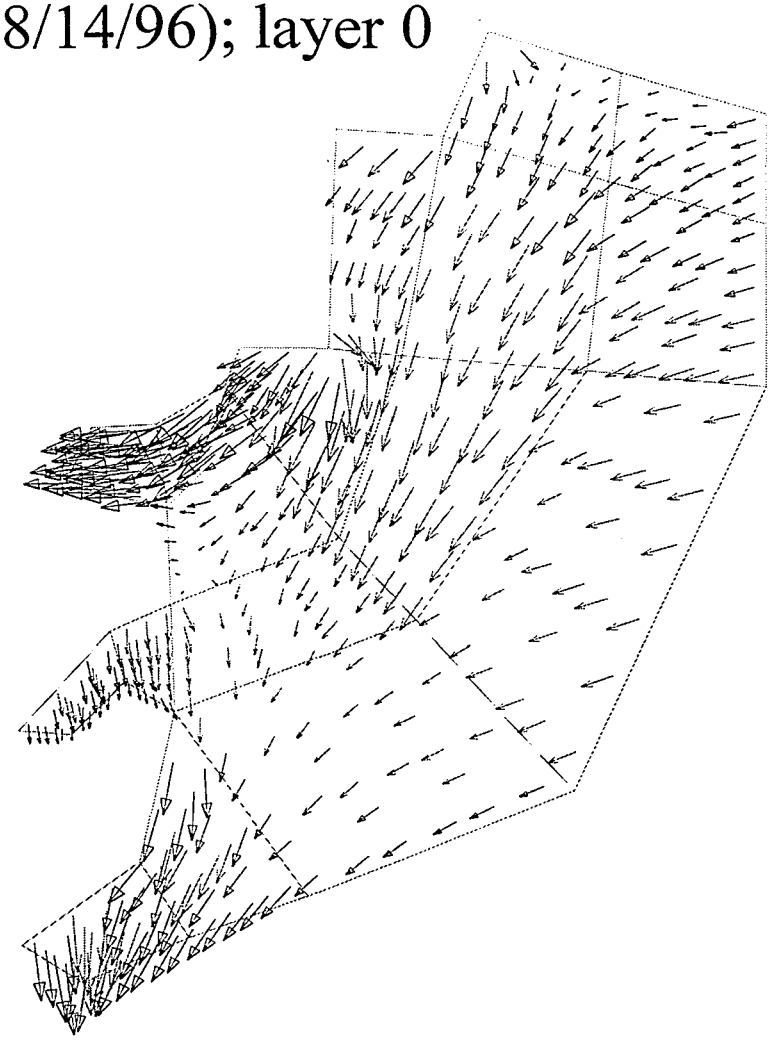

is 26.3842

105 days after start (8/14/96); layer 1 [new data]

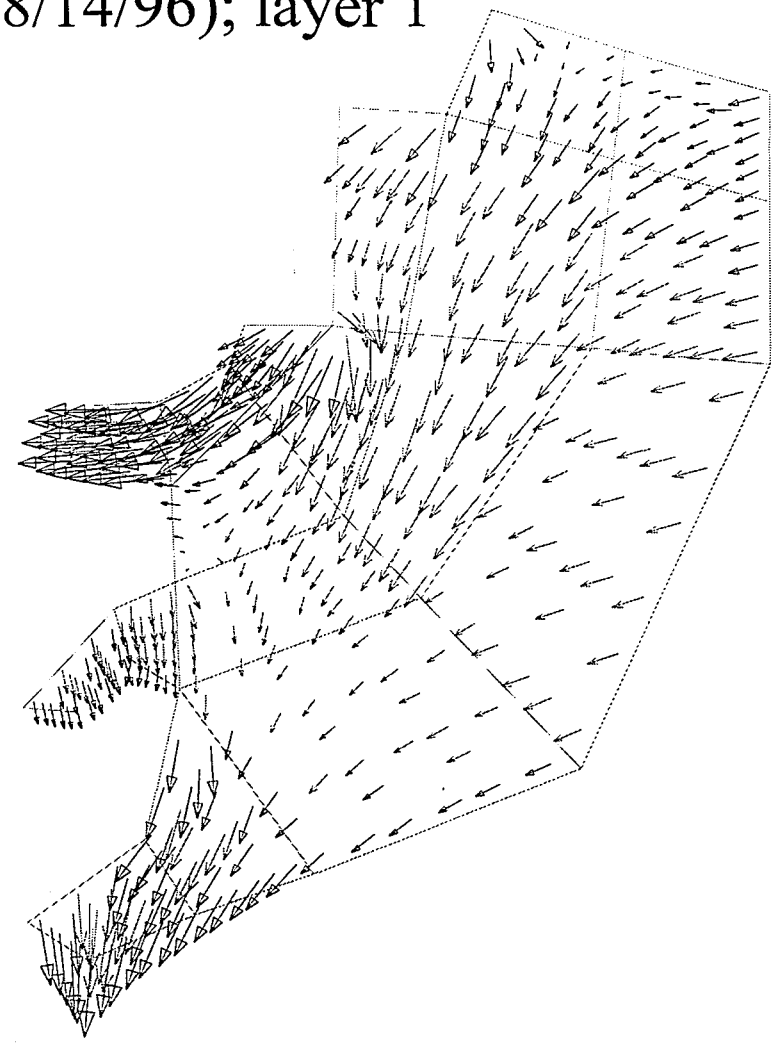

is 26.3842

105 days after start (8/14/96); layer 2 [new data]

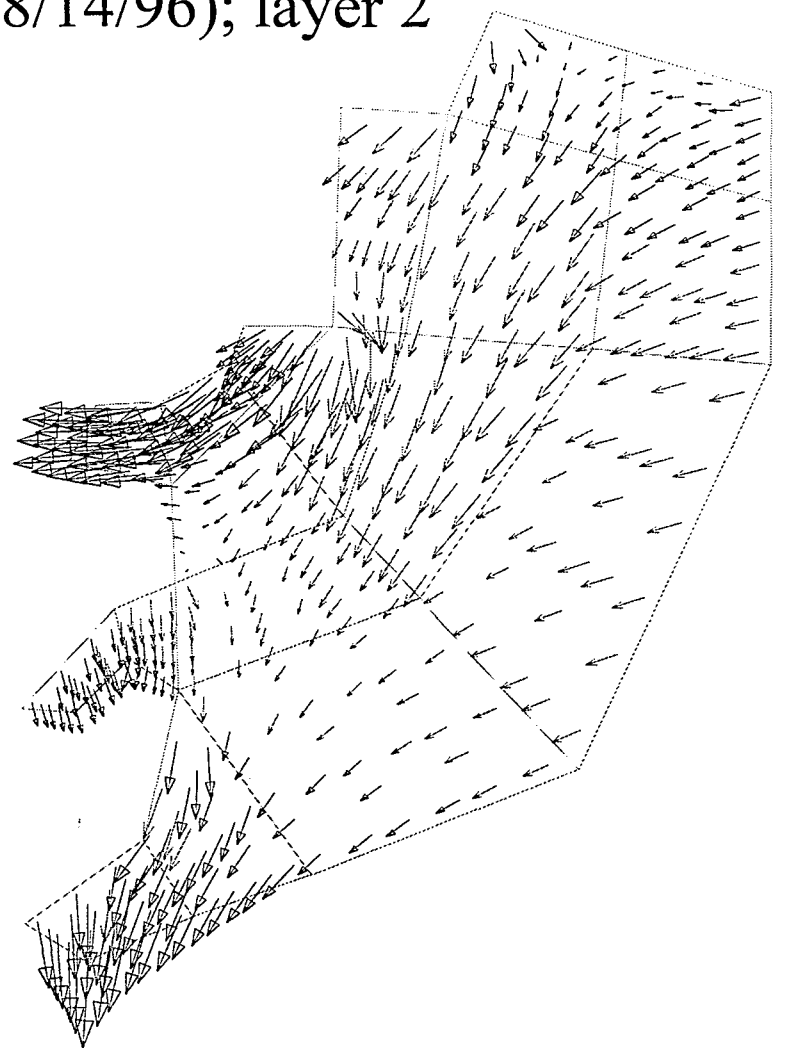

is 26.3842

105 days after start (8/14/96); layer 3 [new data]

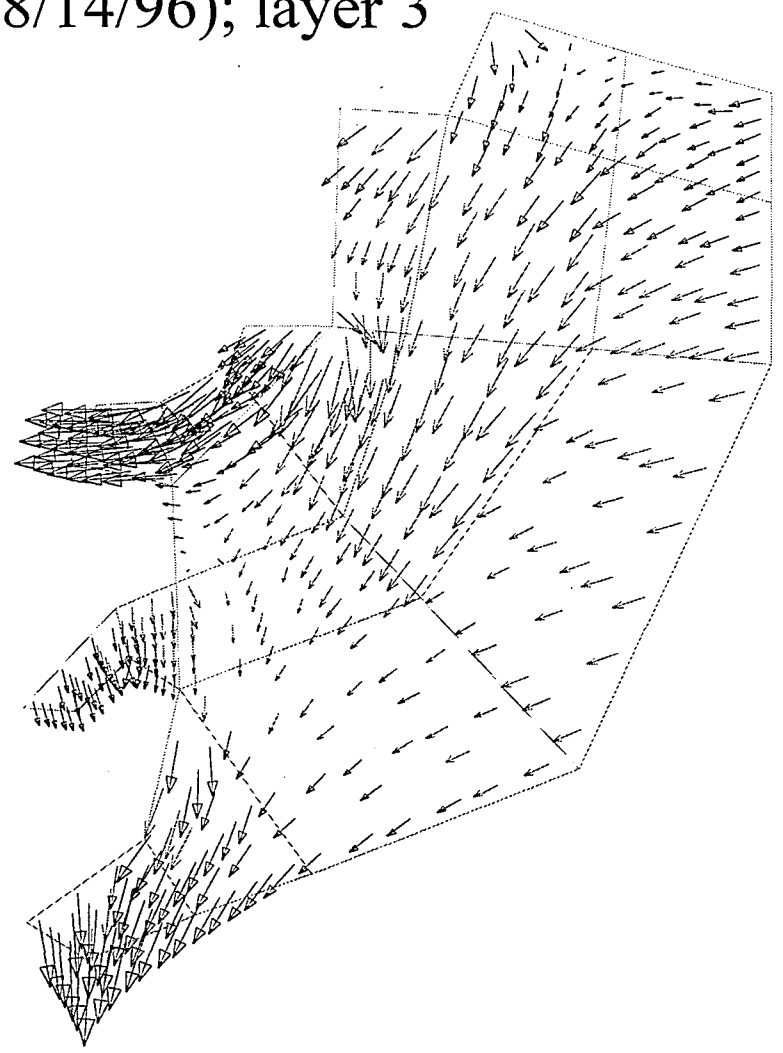

is 26.3842

105 days after start (8/14/96); layer 4 [new data]

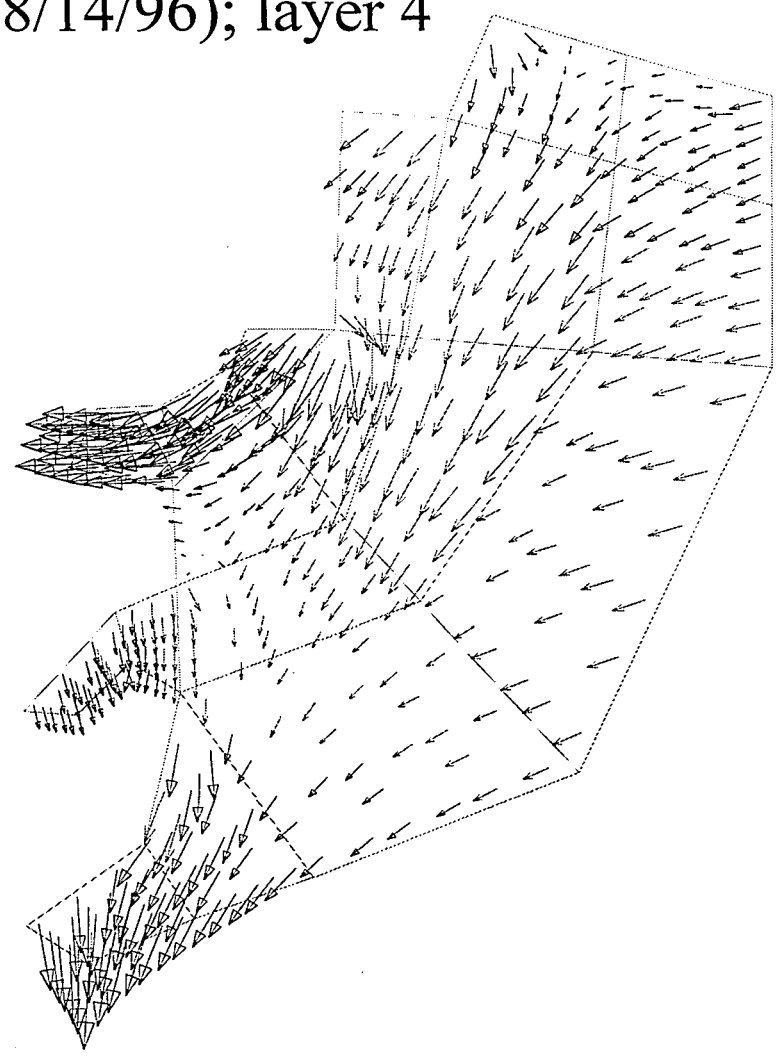

is 26.3842

105 days after start (8/14/96); layer 5 [new data]

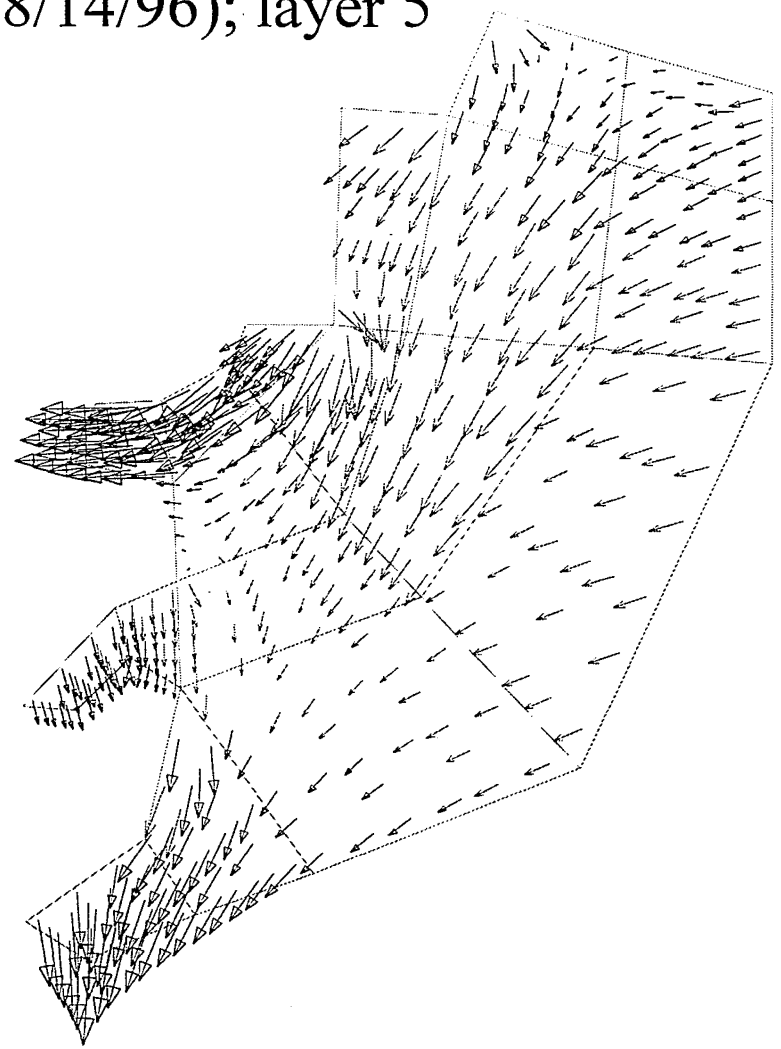

is 26.3842